KfK 3756
August 1984

Influence of Gradual Density Transition and Nonlinear Saturation on Rayleigh-Taylor Instability Growth

H. Jacobs
Institut für Neutronenphysik und Reaktortechnik

Kernforschungszentrum Karlsruhe

KERNFORSCHUNGSZENTRUM KARLSRUHE

Institut für Neutronenphysik und Reaktortechnik

KfK 3756

Influence of Gradual Density Transition and Nonlinear Saturation on Rayleigh-Taylor Instability Growth

H. Jacobs

Kernforschungszentrum Karlsruhe GmbH, Karlsruhe

Kernforschungszentrum Karlsruhe GmbH
ISSN 0303-4003

Abstract

Linear theory of Rayleigh-Taylor instability growth at a density profile which varies exponentially between regions of constant density is discussed in detail. The exact theory provides an approximate but conservative simple formula for the growth constant and it shows that a hitherto widely used theory erroneously underestimates the growth constant.

A simple but effective "synthetical model" of nonlinear bubble growth is obtained from a synthesis of linear theory and constant terminal bubble speed. It is applied to pusher shell break-up in an inertial confinement fusion pellet to determine the maximum allowable initial perturbations and the most dangerous wavelength. In a situation typical of heavy ion drivers it is found that the allowable initial perturbations are increased by a few orders of magnitude by the gradual density transition and another order of magnitude by nonlinear saturation of the bubble speed. The gradual density transition also shifts the most dangerous wavelength from about once to about four times the minimum pusher shell thickness.

The following topics are treated briefly: Reasons conflicting with use of the synthetical model to decide whether the pusher shell in a certain simulation will be broken up; other nonlinear theories available in the literature; further realistic effects that might aggravate instability growth.

Einfluß von stetiger Dichteänderung und nichtlinearer Sättigung auf das Wachstum von Rayleigh-Taylor Instabilitäten

Zusammenfassung

Die lineare Theorie der Rayleigh-Taylor Instabilität an einem Dichteprofil, das zwischen Gebieten konstanter Dichte einen exponentiellen Anstieg aufweist, wird ausführlich diskutiert. Die strenge Theorie liefert eine einfache aber konservative Näherungsformel für die Wachstumskonstante und sie zeigt, daß eine bisher weithin benutzte fehlerhafte Theorie die Wachstumskonstante unterschätzt.

Durch Aneinanderfügung der linearen Theorie und einer konstanten Blasengrenzgeschwindigkeit wird ein einfaches aber nützliches "kombiniertes Modell" des nichtlinearen Blasenwachstums gewonnen. Es wird angewendet auf die Bestimmung von maximal erlaubten Anfangsstörungen und gefährlichster Wellenlänge im Fall des Aufbruchs der Pusherschale in einem Brennstoffkügelchen für Kernfusion durch Trägheitseinschluß. In einer für Schwerionentreiber typischen Situation ergibt sich, daß die zulässigen Anfangsstörungen durch die stetige Dichteänderung um einige Größenordnungen und durch die nichtlineare Sättigung der Blasengeschwindigkeit um eine weitere Größenordnung vergrößert werden. Die stetige Dichteänderung verschiebt außerdem die gefährlichste Wellenlänge vom Einfachen auf etwa das Vierfache der minimalen Dicke der Pusherschale.

Folgende Themen werden kurz behandelt: Gründe, die der Anwendung des kombinierten Modells auf die Entscheidung ob die Pusherschale in einer bestimmten Simulation aufbricht oder nicht, entgegenstehen; andere nichtlineare Theorien in der Literatur; weitere realistische Effekte, die das Wachstum der Instabilitäten beschleunigen könnten.

Table of contents

	page
1. Introduction	1
2. Linear theory of Rayleigh-Taylor instabilities	7
2.1 General equations	7
2.1.1 Statement of the problem and historical review	7
2.1.2 Basic equations	8
2.1.3 Remarks	10
2.1.4 Transition to nondimensional variables	11
2.1.5 Boundary conditions	11
2.2 Superposed liquids of constant densities	12
2.3 Free surfaces	13
2.4 Remarks	15
2.5 Exponential density transition without free surfaces	16
2.6 Note on general initial conditions	25
3. Estimate of instability growth at gradual density transitions	28
3.1 Introductory remarks	28
3.2 Determination of the growth constant	28
3.3 Less effective bounds of the growth constant	29
3.4 Hitherto used incorrect estimate of growth constant	30
4. Nonlinear bubble growth	35
4.1 The problem	35
4.2 Simple synthetical model	36
4.3 Nonlinear theory of bubble growth	42
4.4 Other nonlinear theories	44

5. Applications to pusher shell breakup 47
5.1 Formulation of the problem 47
5.2 Determination of maximum allowable initial perturbations 49
5.2.1 Numerical example 49
5.2.2 Possible extensions 52
5.3 Most dangerous wavelength 56
5.3.1 Introductory discussion 56
5.3.2 Determination from shortest breakthrough time 57
5.3.3 Determination from smallest maximum allowable initial disturbances 59
5.3.4 Potential effect of reduction of the terminal bubble speed by a gradual density transition 61
5.4 Discussion of effects that could lead to faster instability growth 62
5.4.1 Effect of finite pusher shell thickness 62
5.4.2 Effect of compressibility 64
5.4.3 Effect of three-dimensional disturbances 65
5.4.4 Nonlinear effect of higher harmonics 66

6. Summary and conclusions 68

7. Literature 71

1. Introduction

Rayleigh-Taylor instabilities occur when a boundary between two fluids is accelerated in the direction of the denser fluid. The classical example is a layer of water being suspended by air so that it cannot fall freely. This system is equivalent to one without gravity but an upward acceleration of amount g. Of course, a perfectly flat interface would persist, but any sinusoidal perturbation of wave number k (e.g. any Fourier component of any arbitrary initial disturbance) has been shown to grow as e^{nt}, where $n^2 = gk$, if the density of the air is neglected for the moment. This is a result of linear analysis which is valid for small deviations from a stable state only. The development after this initial "linear" stage is characterized by the fact, that an initially sinusoidal perturbation deviates from this shape and develops into a "bubble and spike" configuration, in which, finally, round ended columns of the lighter fluid (the "bubbles") penetrate the heavier fluid at a constant speed, while spikes of the heavier fluid fall freely through the lighter one.

Among many other and widespread fields in physics as e.g. star formation, dynamics of the ionosphere, drop shattering by shocks, and film boiling, Rayleigh-Taylor instabilities play an important role in inertial confinement fusion. For this special way of attaining thermonuclear burn, extremely high fuel (DT) densities are required. It is hoped to reach them by spherically imploding small spherical pellets containing the fuel. The necessary high pressures shall be produced by depositing highly energetic particles (photons, heavy ions, light ions or electrons) in the outer shell of the pellet. Evaporation of that shell is expected to drive the inner parts of the pellet (the fuel) towards the center where it accumulates and reaches high pressures and densities. In this process, maintenance of spherical symmetry is of crucial importance. One possible source of asymmetries is the growth of any irregularities due to Rayleigh-Taylor instabilities.

There are several occasions during pellet compression, in which Rayleigh-Taylor instabilities can become important. In this report, however, the problem will be discussed with the background of one situation which is of special importance in light and heavy ion fusion: stability of the pusher shell adjacent to the fuel during the inward acceleration of the fuel. As

an illustration, a case obtained by Tahir and Long (1982) simulating performance of a drafted HIBALL pellet with the MEDUSA code will be used. Figure 1 shows the relevant density distributions (on a logarithmic scale). Part a) showing the original configuration makes evident that the pellet consists of a large void surrounded by a single layered shell comprising fuel (DT), pusher (LiPb), and tamper (Pb). Part b) shows the situation about 27 ns after start of the energy deposition on the pellet by the ions. They have heated mainly the pusher so that its outer part expanded, blowing a compressed pusher layer and the fuel inwards. This created a zone (2.65 mm to 2.77 mm) in the pusher where less dense material accelerates denser material. In this region disturbances could grow and distort or even destroy the pusher-fuel interface. In this way pusher material could be mixed with the fuel and prevent its burn even if ignition still were possible. Actually, a thin layer of pusher material adjacent to the fuel remains cold and moves with the fuel forming the so-called payload. Destruction of this pusher shell almost certainly would make ignition impossible. Since a spherically symmetric pellet calculation cannot tell

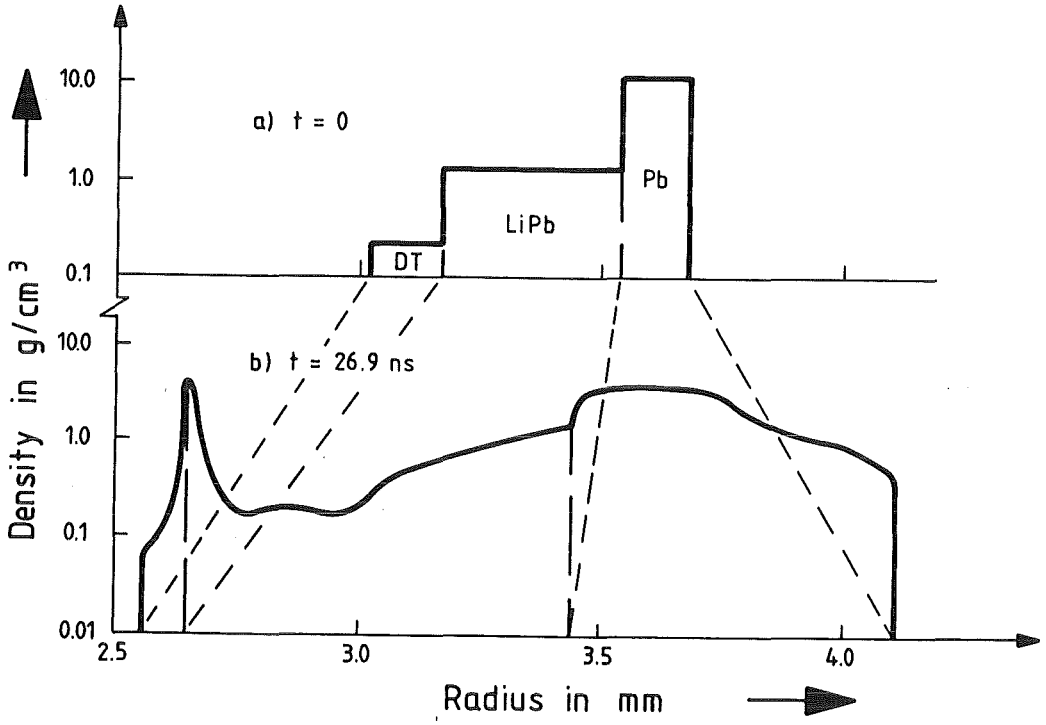

Figure 1: Logarithmic density profiles of HIBALL pellet (Tahir and Long (1982)):
a) initial state
b) unstable situation during compression phase

whether the pusher shell will survive, a separate check is necessary and it is the purpose of this report to discuss a (zero to) first order approach to this question.

Due to the combined actions of continuous ablation and spherical convergence the pusher shell during the acceleration process attains a minimum thickness d and rapidly becomes thicker afterwards. It seems reasonable and has become customary to take this minimum thickness as a measure of the maximum allowable disturbance amplitude. Also, arguments which will be discussed explicitly later in this report show that from all possible sinusoidal perturbations (all wavelengths) those with wavelengths about equal to the amplitude in question are the first to reach this amplitude. So, while no information is yet available on the possible nature of initial disturbances in the pusher shell that could grow due to Rayleigh-Taylor instability, the minimum pusher shell thickness d gives a measure of the most dangerous wavelength and of the maximum allowable amplitude. This report describes how the growth of the most dangerous disturbance can be estimated conservatively on the basis of data obtained from spherical pellet calculations. The method allows to determine a maximum allowable initial perturbation which, at present, essentially must be taken as figure of merit when comparing different pellet designs and/or driver parameters, because there is no reliable figure available to compare the allowable initial amplitude and velocity with.

The above discussion only partly illustrates the complexity of the physical situation in which the pusher shell stability is to be investigated. Simple application of the classical formulae cited above would be inappropriate for a number of reasons:

1. The instability does not occur at an interface between materials of different densities but at a gradual density transition.

2. Under the prevailing conditions, i.e. temperatures of the order of one million Kelvin and pressures of several tens of megabars, the material will behave like an ideal gas with modifications due to degeneracy. To what extent it can be approximated by an incompressible liquid remains to be clarified.

3. In addition to pressure variations, the density of the fluid may be altered by heat addition due to ion deposition, thermal conduction, or thermal radiation.

4. An especially important pressure variation in perpendicular direction is due to heat transport (mainly by radiation) from the wave crests filled with hotter material into the neighbouring troughs containing cooler material. This heat transport is expected to produce a transverse pressure distribution which opposes instability growth.

5. Instead of being due to an external gravitation field or uniform acceleration of the whole system, the acceleration of the pusher shell is due to a positive pressure gradient within the pusher. So, in principle, the "gravitation" to be considered is variable with space in all directions and time.

6. The instability is limited to a small "instability zone" where the gradients of pressure and density have opposite signs. In the adjacent regions the arrangement is stable and impedes instability growth.

7. Due to continuous ablation the instability zone may move towards the fuel-pusher interface. Usually this is expressed differently: the material may flow (convect) through the instability zone from the high-density to the low-density side (from the top to the bottom).

8. Instead of filling the whole half-spaces above and below the density transition zone with homogeneous fluids, respectively, especially "above" the instability there are only limited layers of pusher material and fuel.

9. In reality, the instability occurs at the surface of a sphere. Treating it as flat is a valid approximation for shorter wavelengths only.

10. As real fluids, fuel and pusher material are equipped with surface tension and viscosity.

11. In reality, instabilities may be three-dimensional in nature. While this is neglected in most instances, it may have an influence on the growth rate.

12. Since the test amplitude is of the order of the wave length, it would be inappropriate to use linear theory throughout. It would underestimate considerably the time to reach the test amplitude.

13. Initially, disturbances of different wave lengths may be present. In the linear regime these different modes may be considered separately as they do not interact with each other. In the nonlinear regime, however, the presence of higher harmonics may increase the growth of the fundamental mode.

It appears that full and combined account of all the points listed above requires a full numerical simulation with a two- or even three-dimensional hydrocode. However, due to the expenditure of such calculations, they must be limited in number. Also, it is urgently required to understand the effect of the realistic refinements on the basis of physical considerations - not least to obtain guidance and realistic test cases for the numerical studies. Actually, quite some of the topics are amenable to more or less accurate analysis. It has, for instance, been shown by Suydam (1978) that surface tension is rather unimportant while viscosity could greatly reduce instability growth if it were to increase with pressure as indicated by yet unconfirmed experimental evidence.

In the present report only the first (gradual density transition) and the twelfth topic (nonlinear growth) will be treated, with some comments on effects that may increase the growth rate. In the theoretical studies and the example given, constant acceleration and density gradient will be used. It should, however, be kept in mind, that in a half-analytical procedure, those variables may be re-determined (from a spherical pellet simulation) from time to time, so that quasi-steady variations of them can be covered. In this way, it will be possible to take into account some effects of varying energy deposition (e.g. range shortening, ion energy variation) and other time dependencies in a straight forward manner.

Lewis (1950) has reported three stages of Rayleigh-Taylor instability growth:

1. Stage described by first-order theory (small amplitudes, exponential growth),
2. transition stage,
3. final stage (steadily growing bubbles, freely falling spikes).

Later, Birkhoff (1955) has proposed to consider two further stages:

4. Distortion stage (boundaries between bubbles and spikes are distorted by vorticity and Kelvin-Helmholtz instability),
5. mixing stage (a turbulent mixing zone is formed between the two fluids).

Discussions in this report are limited to the first three stages. They are termed linear, transition and nonlinear stage, respectively. The last two stages need not be considered because the conditions in the envisaged application roughly correspond to Lewis' experiment:

a) The density of the low-density (the blow-off) region is small compared with that of the high-density region (the pusher shell).
b) For definiteness, discussions are largely restricted to a single sinusoidal initial perturbation.
c) Interest is limited to displacement amplitudes of the order of the wavelength (the displacement being measured relative to the virtual undistorted interface or isodensity line). The last two stages can be expected to occur only beyond these amplitudes.

Studying Rayleigh-Taylor instability with neglect of the curvature of the unstable shell appears to be justified since the wavelength considered is of the order of 10 μm while the radius of the shell is of the order of a few millimeters. There are, however, other types of instabilities with wavelengths comparable to the circumference of the sphere that may destroy the symmetry, i.e. the sphericity. It has been demonstrated with numerical simulations by Plesset and Chapman (1971) that a spherical cavitation bubble collapsing close to a wall will deviate from the spherical shape soon and produce a liquid jet projected towards the wall. Furthermore, Fröhlich and Anderle (1980) have observed (e.g. their Figure 3.31) that such jets are formed quite frequently and without close neighbourhood of a fixed wall. This type of instability is, of course, not treated in this report.

In the second chapter the linear theory of Rayleigh-Taylor instability as used later is collected. Chapter three discusses the application of the results for gradual density transitions and in chapter four two approaches to a description of the nonlinear behaviour are presented. Chapter five contains applications and further discussions, and chapter six briefly summarizes the conclusions.

2. Linear theory of Rayleigh-Taylor instabilities

2.1 General equations

2.1.1 Statement of the problem and historical review

This chapter summarizes those parts of linear theory that are of importance for the discussions presented later. It is concerned with inviscid fluids the density of which remains constant with time in any fluid element (e.g. an isothermal and incompressible fluid). Surface tension will be neglected, however, allowance will be made for gradual density variations. Further assumptions are plane geometry in Cartesian coordinates x and z, a constant body force g antiparallel to the z-axis, and small deviations from an equilibrium state in which the fluid is at rest in the coordinate system. One may think of g as being due to a rotation free gravitation field, however, any constant acceleration of the coordinate system in the z-direction just adds to the numerical value of g.

For the "classical" case of discontinuous density variations, the growth rate in the unstable case (the denser fluid above) has been determined by Lord Rayleigh (1883), but is characterized as "known" by him. Also, Lamb (1932) in his Articles 227ff only gives references for the treatment of more complicated cases by Airy and Stokes already around 1840. Later the same result was derived another time by Taylor (1950) for the unstable case and an accelerating system which is fully equivalent to a system at rest but with gravity. He also investigated the influence of a finite depth of the 'upper' fluid layer and initiated the first systematic experimental studies of this instability, Lewis (1950). Therefore, the unstable case, today, is known as Rayleigh-Taylor instability.

The theory of instabilities at gradual density transitions has as well been established by Lord Rayleigh (1883). So, this case is as classical as the one which is usually called so, but apparently, hundred years later, part of Lord Rayleigh's work - exactly the theory needed in the present context - has fallen into oblivion. This may be due to the fact that Lord Rayleigh apparently did not have a means at his disposal to conveniently solve the transcendental equation which is part of the full solution. So, he mainly discussed some limiting cases. His most important explicit

result was that at a gradual density transition the growth rate remains finite when the wave number goes to infinity. Much later, E. Teller proposed the possibility of such a behaviour to LeLevier et al. (1955) who confirmed the speculation by an incorrect theory, see chapter 3. Only recently, the correct theory was rediscovered (or reinvented) and discussed in more detail by three authors: Gerhauser (1980, 1983), Mikaelian (1982), and Kull (1982). The work of Hunt (1961) is less useful due to the approximations used. It appears that the above cited authors were unaware of the fact that the full solution had been supplied by Lord Rayleigh (1883). (Mikaelian's reference to Lord Rayleigh's work is wrong.)

2.1.2 Basic equations

Denoting time as t, pressure as p, density as ϱ, and the Lagrangian coordinates as X and Z so that the velocities in x- and z-direction are $\partial X/\partial t$ and $\partial Z/\partial t$, respectively, the appropriate hydrodynamic equations read (see e.g. Batchelor (1970), p. 174):

$$\frac{\partial^2 X}{\partial x \partial t} + \frac{\partial^2 Z}{\partial z \partial t} = 0 \qquad (2.1)$$

$$\varrho \frac{\partial^2 X}{\partial t^2} + \frac{\partial p}{\partial x} = 0 \qquad (2.2)$$

$$\varrho \frac{\partial^2 Z}{\partial t^2} + \frac{\partial p}{\partial z} + \varrho g = 0 \qquad (2.3)$$

$$\frac{\partial \varrho}{\partial t} + \frac{\partial X}{\partial t} \cdot \frac{\partial \varrho}{\partial x} + \frac{\partial Z}{\partial t} \cdot \frac{\partial \varrho}{\partial z} = 0 \qquad (2.4)$$

As described in detail by Chandrasekhar (1961), pp. 428-30, they can be considerably simplified in the following way: At first all variables are split into their steady-state part (labelled by subscript zero) which they assume in the (presumed) steady equilibrium state and an increment due to the disturbance:

$$p = p_0 + \delta p$$
$$\varrho = \varrho_0 + \delta\varrho$$
$$X = X_0 + \delta X$$
$$Z = Z_0 + \delta Z$$

Insertion of these definitions in (2.1) to (2.4) assuming that $\partial X_0/\partial t = \partial Z_0/\partial t = 0$ and retaining only terms which are at the most linear in the quantities describing the disturbance, gives:

$$\frac{\partial^2}{\partial x\,\partial t}\delta X + \frac{\partial^2}{\partial z\,\partial t}\delta Z = 0 \qquad (2.5)$$

$$\varrho_0 \frac{\partial^2}{\partial t^2}\delta X + \frac{\partial}{\partial x}\delta p = 0 \qquad (2.6)$$

$$\varrho_0 \frac{\partial^2}{\partial t^2}\delta Z + \frac{\partial}{\partial z}\delta p + \delta\varrho \cdot g = 0 \qquad (2.7)$$

$$\frac{\partial}{\partial t}\delta\varrho + \frac{\partial Z}{\partial t}\cdot\frac{\partial}{\partial z}\varrho_0 = 0\,. \qquad (2.8)$$

Furthermore, the solution is sought in terms of normal modes, assuming

$$\delta X = Re\left[s(z)\cdot e^{ikx+nt}\right] \qquad (2.9)$$

$$\delta Z = Re\left[w(z)\cdot e^{ikx+nt}\right] \qquad (2.10)$$

and similar expressions for $\delta\varrho$ and δp, with Re denoting the real part.

Thus, equations (2.5) to (2.8) combine to give

$$\varrho_0 \frac{d^2w}{dz^2} + \frac{d\varrho_0}{dz}\cdot\frac{dw}{dz} + k^2\left(\frac{g}{n^2}\cdot\frac{d\varrho_0}{dz} - \varrho_0\right)w = 0\,. \qquad (2.11)$$

2.1.3 Remarks

It is worth noting that insertion of (2.9) and (2.10) in (2.5) gives

$$S(z) = \frac{i}{k} \cdot \frac{dw(z)}{dz} \quad .$$

Here the imaginary unit i only reflects the 90° phase shift between the components of the displacement: If, e.g. δX behaves as sin kx, δZ behaves as cos kx. The essential point is that δX is proportional to $\partial \delta Z / \partial z$ for all x where δX is not identically zero by virtue of its x-dependence. This means that vanishing of the tangential velocity at a horizontal boundary is equivalent to vanishing of the normal gradient of the vertical velocity. It also means that, along any (vertical) line x = const., the x-components of displacement and velocity change sign when the z-components go through a (local) maximum or minimum. This can lead to a nodal structure of the flow field.

Furthermore, it can be seen that (2.11) only determines n^2, so that both signs of n are allowable. Since (2.11) is linear, any linear combination of e^{nt} and e^{-nt} is a valid solution of (2.11). The coefficients of this linear combination are to be determined from the initial conditions. So, writing the displacement in z-direction which is the only one to be discussed further as

$$\delta Z(x,z,t) = w(z) \cdot \cos kx \cdot h(t)$$

the amplitude h(t) will (in the case $n^2 > 0$) grow as

$$h(t) = h_0 \cosh nt + \frac{\dot{h}_0}{n} \sinh nt \qquad (2.12)$$

where h_0 is the amplitude of the initial displacement and $\dot{h}_0$ the amplitude of the initial disturbance velocity.

For small arguments ($nt \to 0$), cosh $nt \to 1$ and sinh $nt \to nt$ so that in the limit $nt \to 0$ (2.12) becomes

$$h(t) = h_0 + \dot{h}_0 \cdot t$$

which was referred to as initial impulse approximation by Harlow and Welch (1966) since they considered the initial velocity perturbation as the result of an impulsive acceleration at time zero. This relation describes the early time behaviour of any disturbance and, as pointed out by Baker and Freeman (1981), the behaviour of systems without acceleration for which n = 0. For this case, the above linear growth law has first been derived by Richtmyer (1960). It is strictly true for incompressible fluids and Richtmyer has shown that it can also be applied to the case of compressible fluids where the initial velocity disturbance is created by a shock passing in normal direction through an undulated interface between the fluids.

2.1.4 Transition to nondimensional variables

Now, the nondimensional coordinate

$$\zeta = kz \tag{2.13}$$

is introduced, differentiation with respect to this coordinate is denoted by a prime and (the square of) a nondimensional growth constant is defined by

$$\gamma = \frac{n^2}{gk} \tag{2.14}$$

In this way (2.11) becomes

$$w'' + \frac{\rho_0'}{\rho_0} w' - \left(1 - \frac{1}{\gamma} \cdot \frac{\rho_0'}{\rho_0}\right) w = 0 . \tag{2.15}$$

2.1.5 Boundary conditions

The kinematical condition on w is that it must be continuous everywhere. If the geometry is unbounded, $|w| \to 0$ for $|\zeta| \to \infty$ is required in order that the kinetic energy be finite. A further condition which w has to

fulfill at any boundary, at $\xi = \omega$ say, can be derived by integrating (2.15) from $\omega - \varepsilon$ to $\omega + \varepsilon$ and taking the limit $\varepsilon \to 0$. With the definitions

$$\sigma(\omega^-) = \lim_{\varepsilon \to 0} \sigma(\omega - \varepsilon)$$

$$\sigma(\omega^+) = \lim_{\varepsilon \to 0} \sigma(\omega + \varepsilon)$$

where $\varepsilon > 0$ and $\sigma = \rho_0$ or w, and

$$\rho_0(\omega^-) = \rho_1^*$$

$$\rho_0(\omega^+) = \rho_2^*$$

this gives

$$\rho_2^* w'(\omega^+) - \rho_1^* w'(\omega^-) + \frac{1}{\gamma} w(\omega)(\rho_2^* - \rho_1^*) = 0 . \quad (2.16)$$

The equations (2.15) and (2.16) together with the conditions on w listed after (2.15) fully contain the stability problem described in the beginning of this chapter. However, analytical solutions are available for special cases only.

2.2. Superposed liquids of constant densities

A very important case is the "classical" one with

$$\rho_0 = \rho_1 \qquad \xi \leq 0$$

$$\rho_0 = \rho_2 \qquad \xi \geq 0 .$$

In this case ϱ_0' vanishes in both half planes so that, (2.15) reduces to

$$w'' - w = 0$$

in both half planes. So, with an arbitrary constant c

$$w = c \cdot e^{\pm \zeta}$$

are solutions and because they have to vanish as $|\zeta| \to \infty$ one has to choose

$$w = c \cdot e^{\zeta} \qquad \zeta \leq 0 \qquad (2.17)$$

$$w = c \cdot e^{-\zeta} \qquad \zeta \geq 0 \qquad (2.18)$$

where use of the same constant c in both half planes ensures continuity of w at $\zeta = 0$. From (2.17) and (2.18) one obtains that

$$w'(0^-) = w(0)$$

$$w'(0^+) = -w(0)$$

so that (2.16) with $\omega = 0$, $\varrho_1^* = \varrho_1$, and $\varrho_2^* = \varrho_2$ gives the "classical" growth rate

$$\gamma = \frac{\varrho_2 - \varrho_1}{\varrho_2 + \varrho_1} = A \qquad (2.19)$$

which is called the Atwood ratio A.

2.3 Free surfaces

Next, the case of an unstable free surface is considered, i.e. the case

$$\varrho_0 = 0 \qquad \zeta \leq 0$$

$$\varrho_0 > 0 \qquad \zeta \geq 0,$$

hence $\varrho_1^* = 0$ and $\varrho_2^* > 0$.

Then (2.16) gives as the free boundary conditions

$$y \cdot w'(0^+) = - w(0) \tag{2.20}$$

from which

$$y = - \frac{w(0)}{w'(0^+)} .$$

Rewriting (2.15) as

$$w'' - w + \frac{\varrho_0'}{\varrho_0} \left[w' + \frac{1}{y} w \right] = 0,$$

it can be seen that the former solution (2.18) solves the problem for any density distribution $\varrho_0(\xi)$, $\xi > 0$.

Because it gives

$$w' = - w \qquad \text{for all} \quad \xi \geq 0 ,$$

$y = 1$ and the two terms within the brackets cancel each other. This reduces the differential equation (2.11) again to

$$w'' - w = 0$$

which is solved by (2.18), but this time without assumptions on ϱ_0.

Mikaelian (1982) has demonstrated explicitly that the solution (2.18) still holds when density steps are present at some $\omega > 0$: For any density difference $\varrho_2^* - \varrho_1^*$, the boundary condition obtained from (2.16) is

$$y \cdot w'(\omega) = - w(\omega) \tag{2.21}$$

resembling the free boundary condition (2.20), if $w(\xi)$ and $w'(\xi)$ are continuous at the position ω which certainly is the case with (2.18). Since

$y = 1$ and (2.18) gives

$$w' = -w \qquad \text{for all } \xi \geq 0,$$

any number of arbitrary density steps is allowed.

The same considerations apply to the case of a stable free surface, where (2.17) gives

$$w' = w \qquad \text{for all } \xi \leq 0$$

so that (2.16) with $\varrho_2^* = 0$ gives $y = -1$.

2.4 Remarks

Before continuing with gradual density variations, it may be worth to note (Mikaelian (1982), Kull (1982)) that the flow fields discussed above are often called surface modes or (in the stable case) gravity waves. For each wave number and surface there is just one mode of this type. These modes are irrotational. The physical reason for this is that in a homogeneous nonviscous fluid rotation is a conserved quantity. The initial state with the fluids at rest is free of rotation. So, in the regions of constant density and without viscosity which could produce rotation, the flow field remains irrotational. However, in the case of two superposed fluids the tangential velocities at the material interface in which the two irrotational flow fields contact each other have opposite directions so that in this line rotation is infinite. As will become clear in the next section, this does not remain so for instability modes in a gradual density transition. In that case neither the density variation nor the rotation is concentrated in a singular line but fills the whole region with variable density. These instability modes are called internal modes because they result from antiparallel gradients of density and pressure within the interior of a fluid body. They exhibit closed flow paths similar to convection cells. As mentioned by Lord Rayleigh (1883) and most explicitly discussed by Gerhauser (1980, 1983) there exist for any wave number infinitely many higher modes which show ever increasing numbers of layers of such flow cells but grow ever slower.

As shown in the last section, surface modes occurring at a free surface have the striking property that the growth constant (or oscillation frequency) does not depend on the density profile within the fluid. Nor does it depend on the compressibility of the fluid, as mentioned by Kull (1982).

It should be noted that the surface mode originating from a free surface is only a partial solution to the problem, if the density of the fluid is variable. In that case, the full solution will be a linear combination of the free surface mode and other surface modes (if density steps are present) and internal modes (if density gradients occur). In this way the overall growth rate will depend on the whole density distribution. An example of this will be discussed in subsection 5.4.1.

Among all unstable modes the free surface mode will grow the fastest. Therefore, in any problem with an unstable free surface, instability growth is dominated by the free surface mode. This statement may be questionable under very special initial conditions, but such special cases need not be considered here. The matter has been discussed extensively by Mikaelian (1983a,b).

Surface modes with a growth rate which is independent of the density variation within the fluid have also been found at the outer surface of spherically imploded shells by Kidder (1976) and, under more general assumptions, by Book and Bernstein (1980). The latter call only this mode a Rayleigh-Taylor mode and term the internal modes convective modes.

2.5 Exponential density transition without free surfaces

The growth rates of instabilities at an exponentially increasing density profile

$$\varrho_0(\xi) = \varrho_1 e^{\beta\xi} \qquad 0 \leq \xi \leq \Delta \qquad (2.22)$$

were first determined by Lord Rayleigh (1883) under different boundary conditions. The case with flat plates at $\xi = 0$ and $\xi = \Delta$ is fully treated in the text book by Chandrasekhar (1961). The general problem has been

reconsidered by Gerhauser (1980, 1983), Kull (1982), and Mikaelian (1982). The appropriate conditions for the present purpose (which have been treated by Lord Rayleigh (1883) and the last three authors) are

$$\varrho_0(\xi) = \varrho_1 \qquad \xi \leq 0 \tag{2.23}$$

$$\varrho_0(\xi) = \varrho_2 = \varrho_1 \cdot e^{\beta\Delta} \qquad \xi \geq \Delta\,. \tag{2.24}$$

In the regions with constant density, solutions similar to (2.17) and (2.18) are appropriate:

$$w(\xi) = c_1\, e^{\xi} \qquad \xi \leq 0 \tag{2.25}$$

$$w(\xi) = c_2\, e^{-(\xi-\Delta)} \qquad \xi \geq \Delta \tag{2.26}$$

For $0 \leq \xi \leq \Delta$ (2.15) reduces to

$$w'' + \beta w' - \left(1 - \frac{\beta}{\gamma}\right) w = 0 \tag{2.27}$$

the general solution of which is

$$w(\xi) = c_3\, e^{\sigma_1 \xi} + c_4 \cdot e^{\sigma_2 \xi} \tag{2.28}$$

where σ_1 and σ_2 are the roots of the characteristic equation

$$\sigma^2 + \beta\sigma - \left(1 - \frac{\beta}{\gamma}\right) = 0 \tag{2.29}$$

so that

$$\sigma_1 + \sigma_2 = -\beta \tag{2.30}$$

$$\sigma_1 - \sigma_2 = 2\sqrt{D} \tag{2.31}$$

with $$D = 1 + \beta^2/4 - \beta/\gamma \; . \tag{2.32}$$

Again, y and thus $\sigma_1 - \sigma_2$ as well as c_3/c_4 have to be determined from the boundary conditions at $\xi = 0$ and $\xi = \Delta$: With $\varrho_0(\xi)$ being continuous, $\varrho_1^* = \varrho_2^*$ and (2.16) requires $w'(\omega^+) = w'(\omega^-)$, i.e. $w'(\xi)$ must be continuous, as $w(\xi)$ must be. Taking into account (2.25) and (2.26) this means:

$$w'(0) \; / \; w(0) = 1 \tag{2.33}$$

$$w'(\Delta) \; / \; w(\Delta) = -1 \; . \tag{2.34}$$

Before determining the unknowns, it is convenient to rewrite (2.28) following Lord Rayleigh (1883). Observing (2.30) and (2.31) as well as

$$\sigma_1 = (\sigma_1 + \sigma_2)/2 + (\sigma_1 - \sigma_2)/2$$

and $$\sigma_2 = (\sigma_1 + \sigma_2)/2 - (\sigma_1 - \sigma_2)/2$$

(2.28) can be rearranged to give

$$w(\xi) = 2\sqrt{-c_3 c_4}\; e^{-\frac{\beta}{2}\xi} \sinh\left(\sqrt{D}\,\xi + \ln\sqrt{-\frac{c_3}{c_4}}\right).$$

With the definitions

$$i\,\frac{\phi}{\Delta} = \sqrt{D} \tag{2.35}$$

$$-i\,\Gamma = \ln\sqrt{-\frac{c_3}{c_4}} \tag{2.36}$$

$$c_0 = -2\sqrt{c_3 c_4} \tag{2.37}$$

this becomes

$$w(\xi) = c_0 \, e^{-\frac{\beta}{2}\xi} \sin\left(\frac{\phi}{\Delta}\,\xi - \Gamma\right) . \qquad (2.38)$$

Now, application of the boundary conditions (2.33) and (2.34) gives:

$$\cot\Gamma = -\frac{\Delta}{\phi}\left(1 + \frac{\beta}{2}\right) \qquad (2.39)$$

$$2\phi\cot\phi = f(\phi) = \frac{\beta^2\Delta^2/4 + \phi^2 - \Delta^2}{\Delta} \qquad (2.40)$$

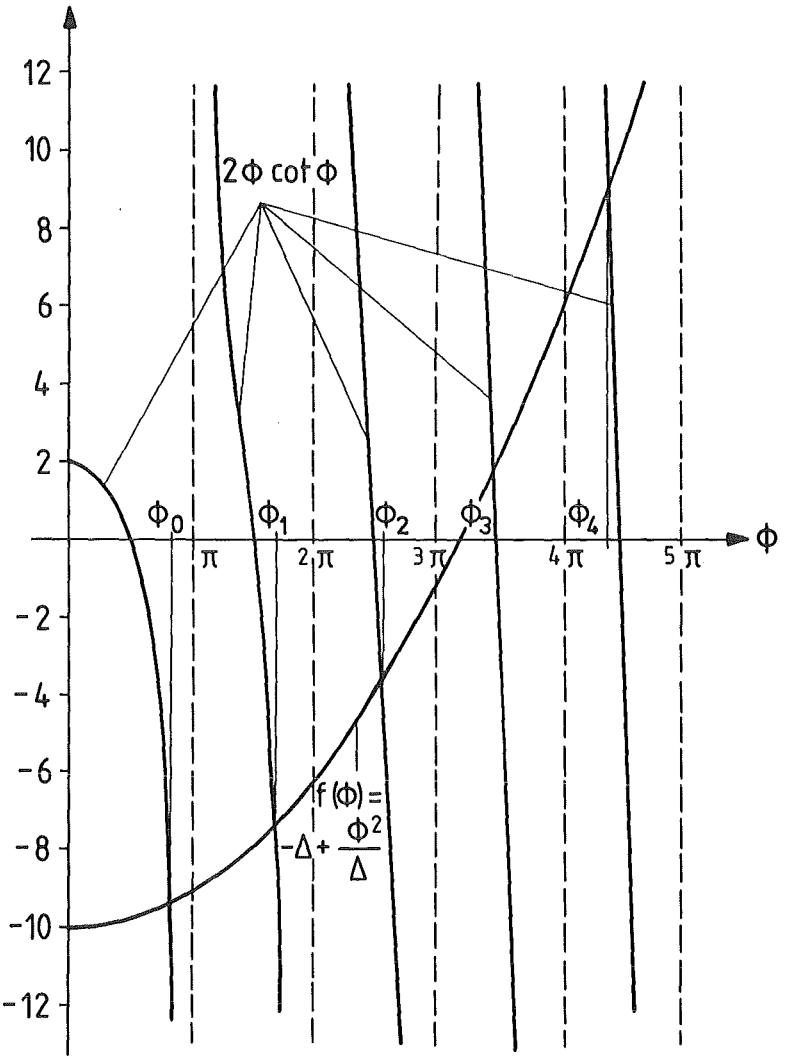

Figure 2: Graphical solution of the transcendental equation (2.40) for $\Delta = 10$ and vanishing β. (After Gerhauser (1980, 1983).)

and knowing ϕ, the growth constant y can be determined after (2.32) and (2.35):

$$Y = \frac{\beta}{1 + \beta^2/4 + \phi^2/\Delta^2} \quad . \tag{2.41}$$

Equations (2.38) to (2.41) together with (2.25) and (2.26) constitute the full solution of the problem (as usual, c_0 remains a free constant and c_1 and c_2 have to be chosen as w(0) and w(Δ) after (2.38), respectively). As demonstrated by Figure 2, (2.40) has infinitely many solutions which correspond to infinitely many instability modes (assuming $\beta > 0$). It is sufficient to consider $\phi > 0$, since (2.40) and (2.41) are symmetric and (2.38) and (2.39) are antisymmetric, so that w(ξ) just changes sign when the negative solution of (2.40) is chosen. The curve f(ϕ) in Figure 2 illustrates the case of $\Delta = 10$ and vanishing β. In this case all solutions are real. This behaviour remains as long as $\beta \leq 2$.

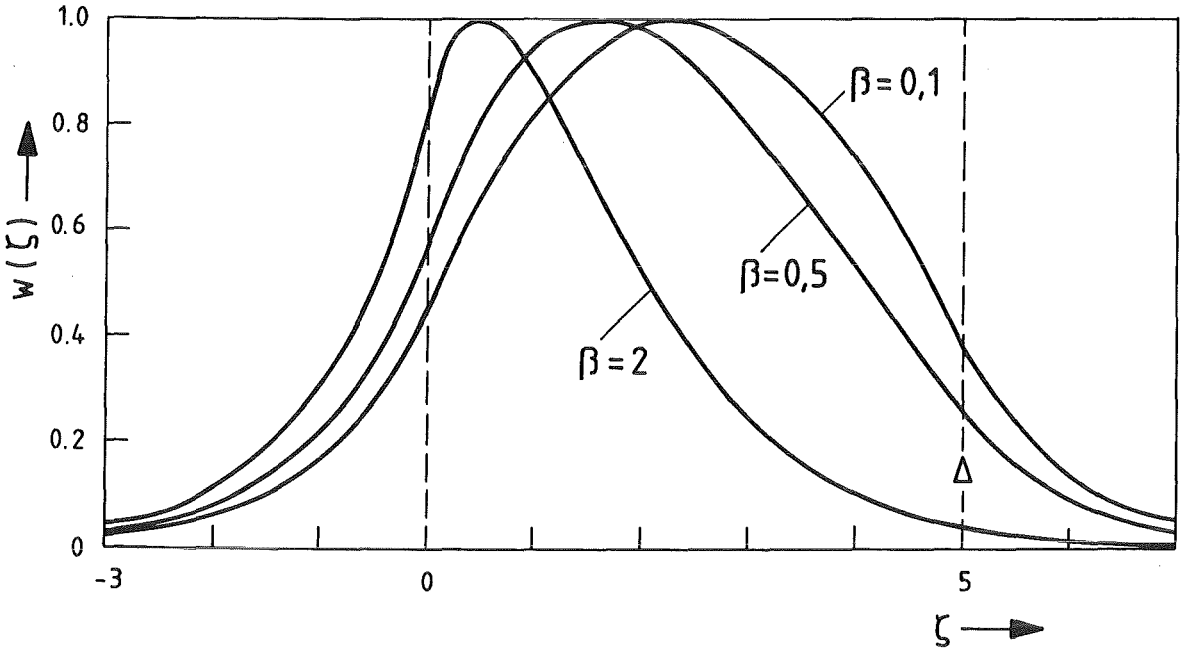

Figure 3: Normalized displacement distributions of the fastest growing mode for $\Delta = 5$. (After Kull (1982).)

For $\beta \leq 2$, one has $0 < \phi_0 < \pi$ for the smallest solution ϕ_0 of (2.40) which according to (2.41) gives the largest growth rate. Then after (2.39) cot Γ

is negative, i.e. $-\pi/2 < \Gamma < 0$. Therefore $\sin(\phi/\Delta \cdot \zeta - \Gamma)$ is positive at $\zeta = 0$. Examples of $w(\zeta)$ are plotted in Figure 3. As already noted by Kull (1982) this type of figure shows that the maximum of the disturbance lies close to the low-density side of the transition region for $\beta \geq 2$ and moves towards the center of that region for decreasing β.

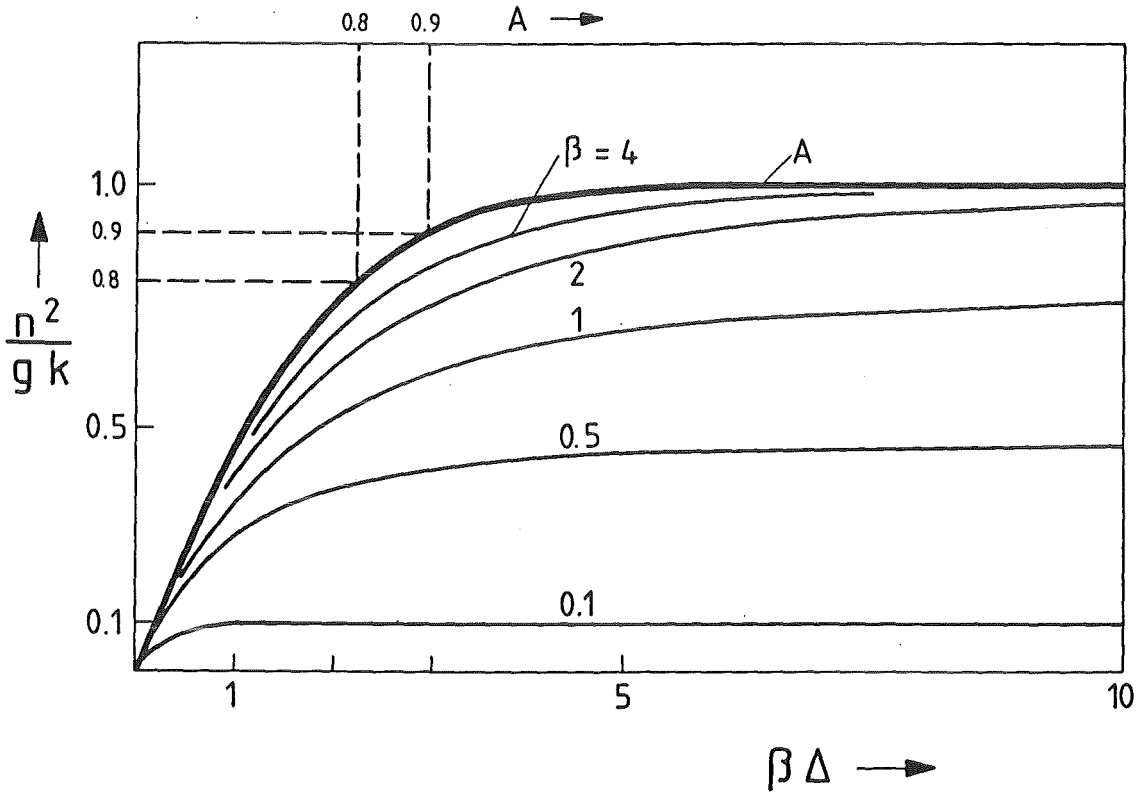

Figure 4: Nondimensional growth constants (squared) for an exponential density transition profile. The thick line represents the classical value (Atwood ratio) valid for step profiles. The growth constants are shown as functions of $\beta\Delta = \ln(\rho_2/\rho_1)$ or the Atwood ratio A (see top fringe). Above $\beta\Delta = 6$, A is very close to 1. (After Kull (1982).)

The nondimensional growth constants (squared) obtained with ϕ_0, i.e. for the fastest growing instability modes, are shown in Figure 4 together with the Atwood ratio A which represents the classical result. The figure

demonstrates that small values of β can considerably reduce the growth constant. For Atwood ratios A close to one the reduction starts to become effective for $\beta \approx 2$. Actually, in the limit $A \to 1$, i.e. $\beta\Delta \to \infty$, $y \to 1$ for $\beta = 2$.

Another way to look at these results is the dispersion relation n(k) the asymptotic value of which can be obtained straightforward: If one considers a fixed density profile with $A \approx 1$ and a certain scale length L of the exponential density variation, one has

$$L = 1/k\beta \tag{2.42}$$

Thus, $k \to \infty$ means $\beta \to 0$. From (2.41) one sees, that for a fixed density distribution (i.e. $\beta\Delta$ fixed so that $\Delta \to \infty$ when $\beta \to 0$) $y \to \beta$ for $\beta \to 0$. Therefore, for $k \to \infty$, the factor y in

$$n = \sqrt{ygk} \tag{2.43}$$

tends towards β, which after (2.42) in 1/Lk. This combines to give

$$n \longrightarrow \sqrt{g/L} \quad , \qquad k \longrightarrow \infty . \tag{2.44}$$

The dispersion relation, calculated after (2.43) is shown in Figure 5 where it is compared with the "classical" dispersion relation $n = \sqrt{gk}$ which would apply to a density step with A = 1. Here the length L has been used to define nondimensional quantities. The figure clearly demonstrates that both growth rates practically agree with each other until Lk = 0.6 i.e. $\beta \approx 1.7$ and that the growth rate at a gradual density transition does not grow beyond the classical value for k = 1/L. This latter result has already been derived by Chakraborty (1975) as discussed in the next chapter.

The cases with $\beta < 2$ are easy to discuss and of main practical interest because of their reduced growth rates. From a theoretical view point, however, it is also interesting to study how the classical behaviour of interfaces is approached when β grows beyond 2, the graphical representation of which is already included in Figure 4. For $\beta > 2$ there is always a (positive) critical value Δ_c of Δ such that

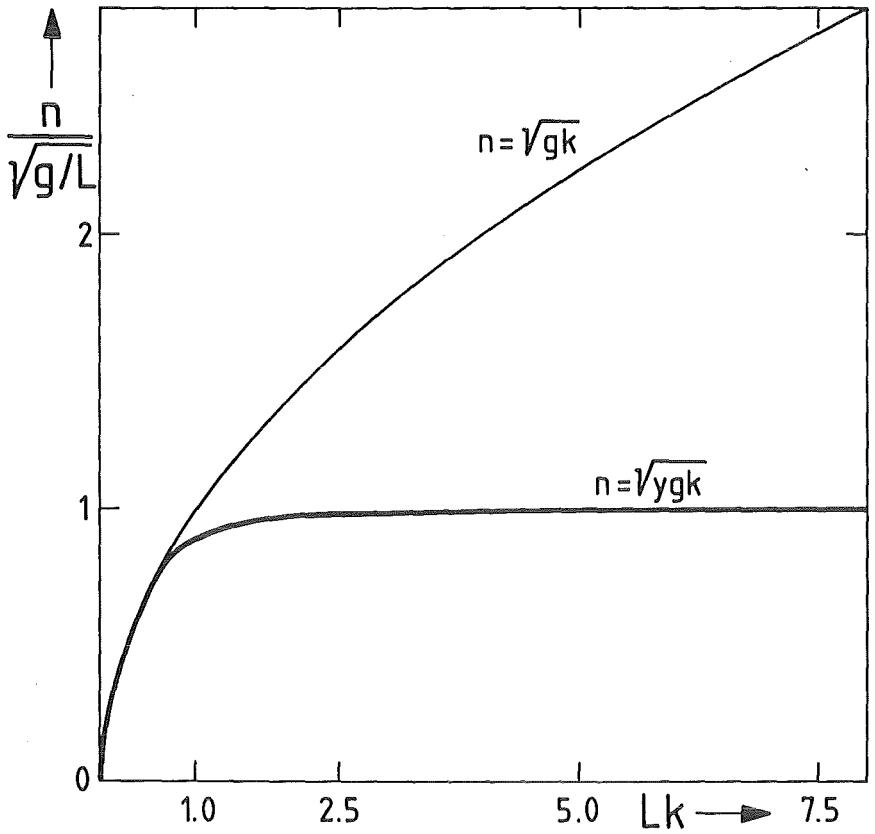

Figure 5: Dispersion relations for a gradual density transition with length scale L and a density step, assuming an Atwood ratio close to one.

$$\beta^2 \Delta_c / 4 - \Delta_c = 2$$

and ϕ_0 becomes zero. (This is the case D = 0 mentioned by Kull (1982).) In the limit $\Delta \to \Delta_c$, (2.38) becomes

$$w(\zeta) = c_0 e^{-\frac{\beta}{2}\zeta} \left(\frac{\zeta}{\Delta_c} + \frac{1}{\Delta_c + \beta \Delta_c / 2} \right) \qquad (2.45)$$

while (2.41) remains valid. Such a case is plotted in Figure 6 for $\beta = 4$ which gives $\Delta_c = 2/3$. With β slightly smaller, the curves are very similar with the maximum slightly shifting to the right as indicated at the top fringe of the figure. It is interesting to note that in the case $\beta = 2$, ζ_{max} here is smaller than for $\Delta = 5$, but is larger in relation to Δ. So, for $\beta \leq 2$, the maximum of the disturbance also moves towards the center of the transition region if the latter grows thinner.

For $\Delta > \Delta_c$, ϕ_0 becomes imaginary. However, equations (2.38) to (2.41) remain valid. Just in terms of the real variables

$$\varphi = \frac{1}{i}\phi \quad \text{and} \quad \gamma = \frac{1}{i}\Gamma$$

the ordinary sine and cotangent are replaced by the corresponding hyperbolic functions. (In his discussion of these different cases, Gerhauser (1980, 1983) disregards the role that β plays and, therefore, erroneously states that ϕ_0 were imaginary for $\Delta < \Delta_c$. This would be true for $\beta < 2$ only, but then $\Delta_c < 0$ which is out of range.)

For $\beta > 2$ and $\beta\Delta \gtrsim 10$, the equations governing the fastest growing mode can be simplified considerably, since in the modified equation (2.40):

$$2\varphi \coth\varphi = \frac{\beta^2\Delta^2/4 - \varphi^2 - \Delta^2}{\Delta} \tag{2.46}$$

$\coth\varphi$ can safely be replaced by one ($\varphi > 0$). (The reason for this is that $2\varphi \coth\varphi$ looks like 2φ essentially, so that φ becomes large as Δ grows.) The solution of the simplified equation is

$$\varphi = (\beta/2 - 1)\Delta \tag{2.47}$$

and equation (2.39) then yields

$$\gamma = \frac{1}{2}\ln\frac{2}{\beta} \quad . \tag{2.48}$$

Furthermore, the location of the maximum can be determined to be

$$\zeta_{max} = \frac{\ln(2 - 2/\beta)}{\beta - 2} \tag{2.49}$$

and (2.38) can be rearranged to give

$$w(\xi) = \frac{c_o}{2}\left[e^{-\xi} - e^{-(\beta-1)\xi} \right] \qquad (2.50)$$

showing that $w(\xi)$ under these conditions can be well approximated by $e^{-\xi}$ except in a narrow region above $\xi = 0$, e.g. $0 < \xi < 2\xi_{max}$. Also, y determined after (2.41) and (2.44) is one. These two results indicate, that the cases which can be approximated in the way just discussed very much resemble the case of superposed fluids of different densities. As an example the case $\beta = 20$, $\Delta = 2/3$ is plotted in Figure 6, which has $\Delta_c = 0.\overline{02}...$ and $\xi_{max} \approx 0.036$. It is seen, that the shape is very similar to $e^{-\xi}$ which is plotted also for comparison.

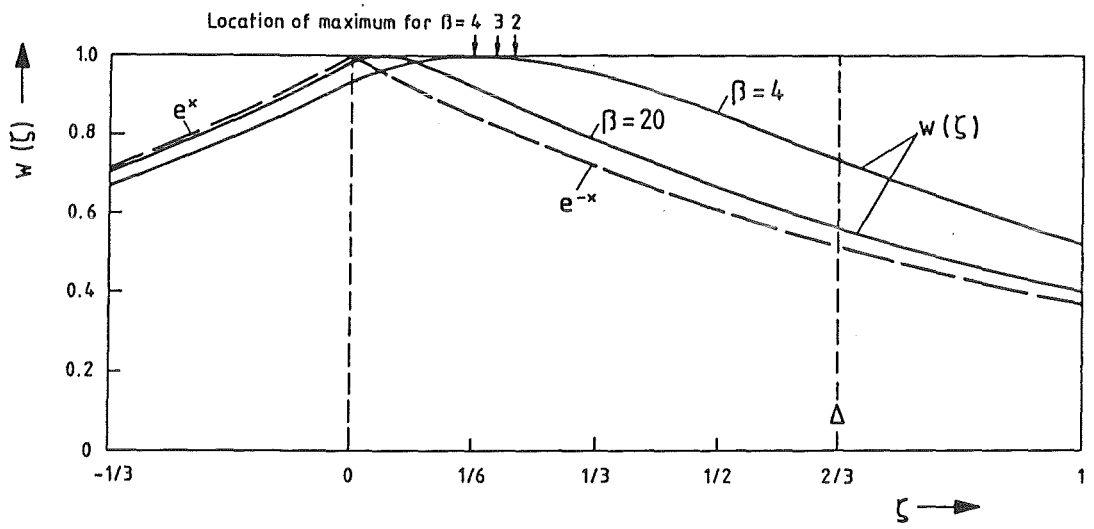

Figure 6: Normalized displacement distributions of the fastest growing mode for $\Delta = 2/3$.

2.6 Note on general initial conditions

In the major part of the literature on Rayleigh-Taylor instability and almost throughout this report a pure sinusoidal initial perturbation is considered. This means that, out of the whole variety of possible instabi-

lity modes (wavelengths) only a single one is studied. Of course, this is possible because any dependence of the initial conditions in x-direction may be Fourier-analyzed and the full result may be obtained by superposition of the individual results for all Fourier components. But it is important to note that this is true in the linear phase only.

When gradual density transitions are considered instead of a single interface there occurs another complication of the same kind: As indicated in the last section the differential equation (2.27) has infinitely many solutions corresponding to the infinitely many solutions of the transcendental equation (2.40). Hence, for any single wavelength there are now still infinitely many instability modes. Up to now only the fastest growing mode has been discussed. This means that the displacement (in ξ-direction) considered was implicitly assumed to be given by

$$\delta Z(\xi, \xi, t) = h(t) \cdot w_0(\xi) \cdot \cos \xi \tag{2.51}$$

which implies the initial conditions

$$\delta Z(\xi, \xi, 0) = h(0) \cdot w_0(\xi) \cdot \cos \xi \tag{2.52}$$

$$\dot{\delta Z}(\xi, \xi, 0) = \dot{h}(0) \cdot w_0(\xi) \cdot \cos \xi \tag{2.53}$$

where $\xi = kx$, $h(t)$ is given by (2.12) and $w_0(\xi)$ is the characteristic function or eigenfunktion of (2.27) corresponding to the lowest eigenvalue $1/y_0$ determined from ϕ_0. Even if the right ξ-dependence is assumed, a general initial condition will differ from (2.52) and require expansion after a complete set of orthonormal functions. That the eigenfunctions $w_i(\xi)$ have the required properties is most easily seen by verifying that the differential equation (2.27) together with the boundary conditions (2.33) and (2.34) and the definition (2.22) constitutes a Sturm-Liouville system, see e.g. Ince (1926), Articles 10.6 ff and 11.5 ff. From this and in particular $\varphi_0'(\xi) > 0$ follows immediately:

a) There exists an infinite set of real and positive eigenvalues which can be arranged in increasing order of magnitude such that

$$1/y_0 < 1/y_1 < \ldots$$

and which tends towards infinity.

b) If the corresponding eigenfunctions are w_0, w_1, ..., then w_m has exactly m zeros in the interval $0 < \xi < \Delta$.

c) The eigenfunctions form an orthonormal set.

d) Any continuous function on $0 \leq \xi \leq \Delta$ which obeys the boundary conditions may be expanded into an infinite series of the eigenfunctions which converges absolutely and uniformly towards the function. Such a Sturm-Liouville development is completely equivalent to a Fourier cosine development.

The increasing number of zeros of the solutions $w_i(\xi)$ means the existence of an increasing number of nodal planes separating individual layers of flow cells. At the elevations of the intervening maxima or minima the horizontal displacements will vanish as discussed in 2.1.3.

Since any initial disturbance naturally fulfills the assumptions of d), it can be decomposed into the components corresponding to the eigenfunctions. Thus, from any actual initial disturbance the "effective" initial disturbance at any elevation may be found, i.e. the initial disturbance that will grow with the growth constant of the fastest growing mode. All higher modes grow so much slower that they should really be of no concern. (Of course, this may be different for different density profiles.)

3. Estimate of instability growth at gradual density transitions

3.1 Introductory remarks

As discussed in the introduction, instabilities of the pusher shell grow in the presence of a gradual density transition. Such a situation has been treated in the previous chapter and the results will be utilized here although the actual density profile may differ considerably from the assumed exponential profile. However, to the writer's knowledge there is only one other type of density profile which has been correctly treated analytically: Lamb (1911) studied oscillations (and by the same token instabilities) in an adiabatic and compressible atmosphere of finite height assuming a constant density gradient. But he applied boundary conditions which prevent use of his results in the present context: a flat plate at the bottom and a free boundary at the top. Only recently, Mikaelian (1982, 1983, 1984) has developed an algorithm which allows to study instability growth at arbitrary density profiles by approximating them with a step profile.

3.2 Determination of the growth constant

It has been shown in the last chapter that an (exponential) gradual density transition with a logarithmic derivative β can lead to an important reduction in growth rate (as compared to the classical value $y = A$ which applies to density steps), if β is much smaller than 2. In the example given by Tahir and Long (1982), which will be presented in detail in the next chapter, $\beta \approx 0.2$ and the growth constant is reduced by about a factor $\sqrt{5}$ which means that the effect is really important in cases of practical interest.

Knowing β and Δ, the (nondimensional) height of the transition zone, y can be determined by solving equations (2.40) and (2.41). It is, however, in many cases of practical interest possible to avoid the solution of the transcendental equation (2.40). To this end, (2.41) is replaced by its limit for $\Delta \to \infty$ which is

$$y^* = \frac{\beta}{1 + \beta^2/4} \quad . \tag{3.1}$$

This y* is an upper bound of y for all $\beta \leq 2$ and y* = 1 for $\beta \geq 2$. Figure 4 shows that in many cases (e.g. $\beta < 1$, $A > 0.95$) one does not lose much by using this much simpler approximation. It is important to note that (3.1) provides a conservative estimate of the growth constant. It is therefore to be preferred to another approximation equally valid for $\Delta \to \infty$, in which ϕ in the denominator of (2.41) is replaced by π (Kull (1982)). That approximation, while having the advantage of still depending on Δ, always underestimates the growth constant. This can be seen from Figure 2 which shows that the lowest ϕ is always smaller than π.

3.3 Less effective bounds of the growth constant

As a corollary from Lord Rayleigh's (1883) work, Chakraborty (1975) determined that

$$y < \beta \tag{3.2}$$

and $y \to \beta$ for $k \to \infty$, i.e. $\beta \to 0$ and $\Delta \to \infty$ while $\beta\Delta$ fixed. Comparison with (3.1) or Figure 4 shows that this is an effective upper bound for small and large $\beta\Delta$, but only in this range. However, (3.2) is valid in the whole range of β and Δ so that for $\beta\Delta < 1$ one may obtain

$$y < \frac{1}{\Delta} \qquad (\beta\Delta < 1) \tag{3.3}$$

which for small β may be an upper bound which is more efficient than the general relation (see Kull (1982))

$$y < A < \beta\Delta/2 \tag{3.4}$$

the second part of which can be helpful for $\beta\Delta < 2$ and large β. Actually, (3.3) and sometimes even (3.4) may give lower but still conservative

estimates of y than (3.1). But this holds for small Atwood ratios only. These are not of practical interest in the present context and, therefore, these bounds are catagorized as less effective, here.

For the case of an exponentially varying density, i.e. for β constant in space, (3.2) and (3.3) are the inequalities which Gamalii et al. (1980) without any argument and without requiring β = const give as their equation (5) in which, apparently, the conditions have been interchanged erroneously.

An "elementary, illuminating, and rigorous" proof of such an inequality in which β is replaced by the maximum that $\partial/\partial\zeta(\ln\varrho_0)$ assumes has been announced by Frese (1982). His further statement that the corresponding instability modes "act only in a thin layer near the mininum of ϱ_0/ϱ_0' " appears questionable in the light of the discussions at the end of the preceding chapter. It may be true for $k \to \infty$ only and, therefore, of little practical use.

3.4 Hitherto used incorrect estimate of growth constant

The theory on which the above outlined estimate of the instability growth rate is based was published by Lord Rayleigh (1883) more than a hundred years ago. Nevertheless, to the present author's knowledge, it has not been used in the present context up to now. Instead, a growth rate estimate due to LeLevier, Lasher and Bjorklund (1955) has been widely used: Bangerter et al. (1975), Bangerter and Meeker (1977), Hussey and McDaniel (1981), Pert (1981), Targove (1981), Tahir and Long (1982), Jacobs (1983).

LeLevier et al. (1955) have considered the antisymmetric density profile

$$\varrho_0 = \varrho_2 - (\varrho_2 - \varrho_1)/2 \cdot e^{-\beta\zeta} \qquad \zeta \geq 0 \qquad (3.5)$$

$$\varrho_0 = \varrho_1 + (\varrho_2 - \varrho_1)/2 \cdot e^{\beta\zeta} \qquad \zeta \leq 0 \qquad (3.6)$$

which is plotted in Figure 7a. In Figure 7b the exponential profile (2.22) to (2.24) is plotted for comparison. Starting from the basic equation (2.3) and assuming separation of variables similar to (2.10)

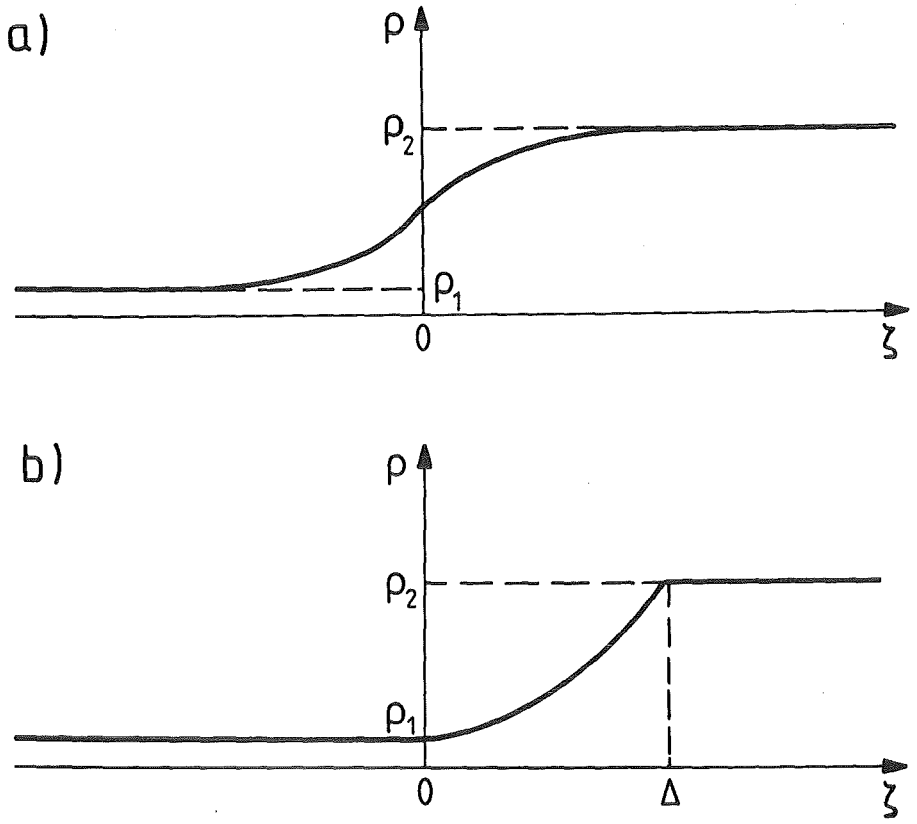

Figure 7: Density transition profiles:
a) antisymmetric
b) exponential

with $$w(\zeta) = c_0 e^{-\zeta} \quad , \qquad \zeta \geq 0 \qquad (3.7)$$

$$w(\zeta) = c_0 e^{\zeta} \quad , \qquad \zeta \leq 0 \qquad (3.8)$$

they determined the time-dependent part of the disturbance velocity by requiring continuity of pressure at $\zeta = 0$. The time-dependent factor turned out to be an exponential function and the growth constant was found to be given by

$$\gamma = \frac{\beta}{\beta + 1} \cdot A \; . \qquad (3.9)$$

In Figure 8 this relation is compared with Lord Rayleigh's result (2.41), showing a more pronounced reduction of the growth constant by the antisymmetric density profile, especially for $\beta = 2$ (and higher values of β). For small β and $A \approx 1$, on the other hand, the results are similar since both, (2.41) or its simpler substitute (3.1) and (3.9) tend towards β for $A \to 1$ and $\beta \to 0$.

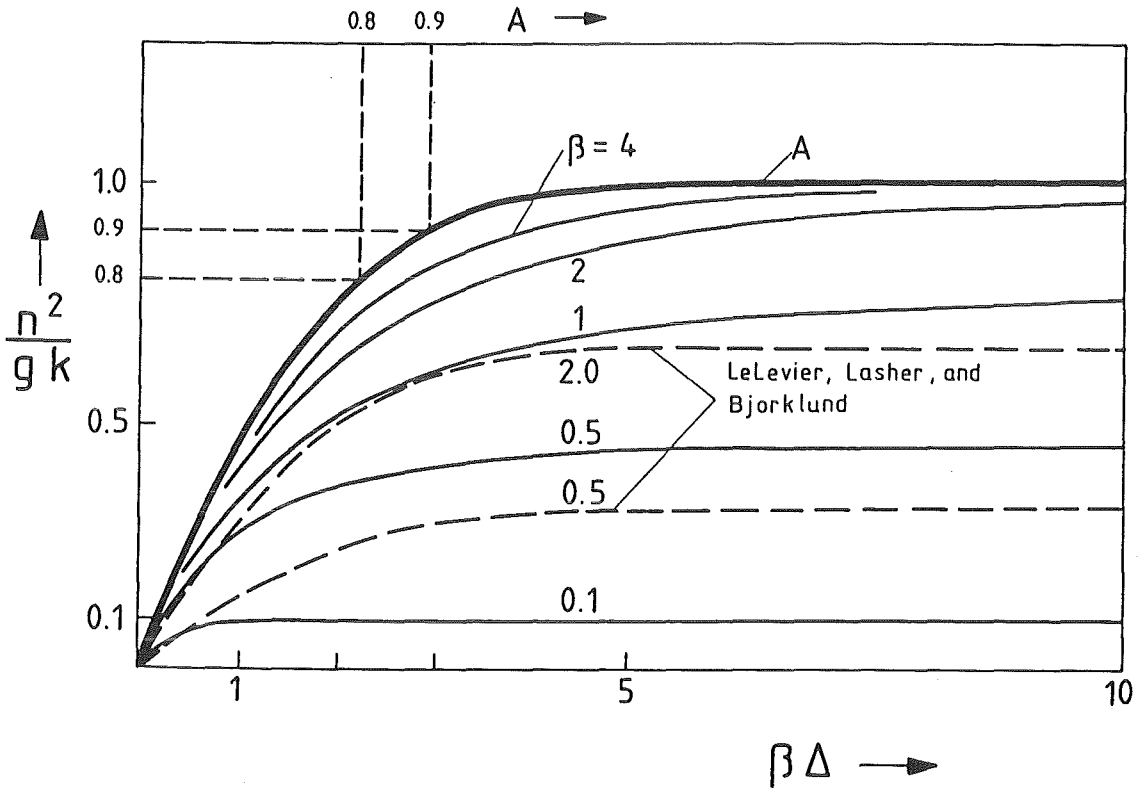

Figure 8: Comparison of the growth constants found by LeLevier et al. (1955) for the antisymmetric profile with Lord Rayleigh's (1883) result for the exponential profile.

Figure 8 does not yet indicate a contradiction since different density profiles (shown in Figure 7) have been considered. It is more serious that, as already pointed out by Targove (1981), the ansatz which was assumed by LeLevier et al. (1955) and which is given here as (3.7) and (3.8) does not fulfill the boundary condition at $\xi = 0$ which for a continuous density profile requires $w'(\xi)$ to be continuous, see the discussion after (2.32). It is difficult to judge to what extent such a formal deficiency influences

the resulting growth rate. However, as demonstrated in chapter 2, the growth rate shows up as an eigenvalue in the differential equation from which the z-dependence of the disturbance velocity is determined, if the instability is analyzed in terms of normal modes. This eigenvalue in turn is determined from the proper boundary conditions. So, the result of LeLevier et al. (1955) must be considered as unreliable.

As a further check, the method of LeLevier et al. (1955) has been applied to the exact solvable problem treated in section 2.5. The result is

$$\gamma = (e^{\Delta(\beta-1)} - 1)\beta\left[(e^{\Delta(\beta-1)}+1)(\beta-1) + e^{\Delta(\beta-1)} - 1\right]^{-1} \qquad (3.10)$$

for $\beta \neq 1$, and

$$\gamma = \Delta/(\Delta+2) \quad , \quad \beta = 1 \qquad (3.11)$$

and it is for $\beta = 0.5$ compared with Lord Rayleigh's result in Figure 9. It is seen that the result of this method can be wrong (to the optimistic side). Therefore, the result of LeLevier et al. (1955), i.e. equation (3.9), should not be relied on further.

It is interesting to note that γ after (3.10) goes to A as $\beta \to \infty$, for all values of $\beta\Delta$. So, (3.10) is the uniform approximation to the step profile result (i.e. A), the absence of which Kull (1982, p. 24) remarks. Actually, a numerical comparison of (3.10) and (3.11) with the correct result obtained from (2.40) and (2.41) shows that (3.10) and (3.11) provide reasonable approximations of the correct result for all $\beta \geq 1$. It can also be observed that for sufficiently large Δ (possibly $\Delta \geq \Delta_c$) the approximation overestimates the growth rate and thus provides a conservative estimate. Nonetheless, (3.10) is of little practical use since all the growth constants so determined are close to A anyhow.

It might be found astonishing that, in the range of $\beta \geq 1$, the ansatz of LeLevier et al. (1955) which is formally inconsistent leads to such rather reasonable results. The reason for this becomes obvious on inspection of Figure 4 which demonstrates that for $\beta > 2$ and $\Delta > \Delta_c$ the correct solution

is well approximated by exponential functions except in a small region above zero where the formal inconsistency occurs.

In the opposite case, $\beta \to 0$, y after (3.10) goes to $\beta/2$, showing that the result is off by a factor of 2 to the optimistic side.

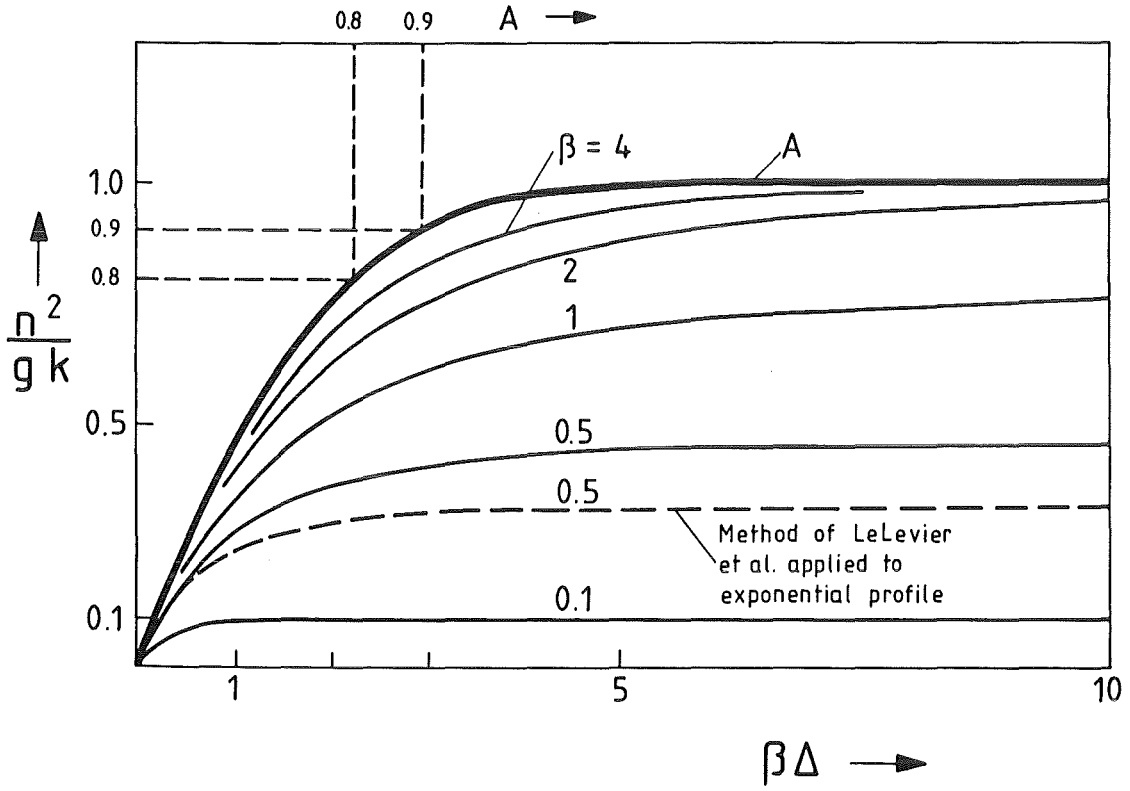

Figure 9: Comparison of the growth constants determined with the method of LeLevier et al. (1955) for the exponential profile with the correct result due to Lord Rayleigh (1883).

4. Nonlinear bubble growth

4.1 The problem

Even under the assumed simplifying conditions linear theory as that presented in chapter 2 describes the growth of an infinitesimally small disturbance only. As the disturbance grows, nonlinear effects (still under the same simplifying assumptions) will start to reduce the growth acceleration. Also, these effects will cause a change in the shape of the disturbance. If it is sinusoidal in the beginning, the crests where the light fluid penetrates the heavier fluid will start to broaden and form round-ended columns or bubbles, while the troughs become increasingly narrow and form spikes of the heavier fluid that "fall" through the lighter medium. (The latter being true for Atwood ratios close to one only, see e.g. Daly (1967)). Since the disturbance amplitudes within the high density material are characterized by the bubble amplitude, only the question of bubble growth is considered further. The important point about this is that the bubble rather quickly assumes a constant 'terminal (or ultimate) bubble speed' $\dot{A}_t$, so that finite bubble amplitudes (larger than some fraction of the wavelength) need much more growth time than linear theory would predict.

The above discussion is qualitatively supported by experimental observation, e.g. Lewis (1950) and Emmons, Chang, and Watson (1959). However, it is difficult to obtain quantitative information from experiments because they suffer from numerous complications as not purely sinusoidal initial perturbations, wall effects, actions of surface tension and viscosity, Kelvin-Helmholtz instability, etc. More reliable quantitative information can be expected from fully numerical simulations. However, apparently for reasons of computational stability, they are often initiated with such high disturbance velocities that linear theory is not applicable, e.g. Harlow and Welch (1966) and Daly (1967). While Daly (1969) has done many calculations in the linear regime, he does not present how the computed growth rates depart from those predicted by linear theory. Such information is provided by Baker, Meiron, and Orszag (1980) and Menikoff and Zemach (1983). Combining the information from these two sources, it can be concluded that in the case of small initial perturbations the bubble growth rate soon starts to increase more leisurely than predicted by

linear theory and approaches the terminal bubble speed by increasing monotonically. Only with larger initial perturbations, the bubble speed may overshoot and exceed slightly the terminal bubble speed for some time. The really nonlinear theories that have been available until recently do not describe correctly the late-time behaviour of instabilities. They are commented upon at the end of this chapter.

Very recently a nonlinear theory has been developed by Kull (1983), which describes bubble growth throughout from the initial linear phase to the late quasi-steady phase and is in excellent agreement with all pertinent information available otherwise. Unfortunately, this theory cannot be made to directly account for the very important effect of growth reduction by gradual density transitions discussed in chapter 3. Therefore, at first, in the next paragraph, a simple synthetical model is presented in which just the linear theory is used until it is reasonable to switch to the terminal bubble speed. After that, the results of Kull's theory are presented and used to check the simple model. Finally, some older nonlinear theories are discussed briefly.

4.2 Simple synthetical model

Numerical simulations, as reported in the last section, indicate that linear theory very soon starts to overestimate bubble growth. They also indicate that under the condition of very small initial perturbations, the bubble growth rate will never exceed the terminal bubble speed observed in experiments and simulations and found theoretically. For such initial conditions, a conservative estimate of the bubble amplitude can be obtained by using linear theory until the so predicted growth rate equals the terminal bubble speed and applying the latter from then on. This model is, therefore, merely a synthesis of two already well known special solutions.

Linear theory predicts the disturbance amplitude in any plane to grow as

$$A(t) = A_0 \cosh nt + \frac{\dot{A}_0}{n} \sinh nt \,. \qquad (4.1)$$

Here (2.12) has been specialized to the bubble amplitude A and the initial displacement amplitude h_0 and the initial velocity amplitude $\dot{h}_0$ are now called A_0 and $\dot{A}_0$, although, in the linear regime, the amplitudes of bubble and (precursor of) spike are equal. In general, the initial disturbances of both, displacement and velocity, will be nonzero. In the absence of reliable information on those disturbances it seems appropriate to assume

$$\dot{A}_0 = n A_0 \tag{4.2}$$

so that (4.1) reduces to

$$A(t) = A_0 e^{nt} \tag{4.3}$$

which resembles the growth law used in many instances but actually, on the basis of a more careful investigation of the time behaviour during the linear phase, implies that an initial displacement amplitude A_0 and an initial velocity disturbance with amplitude nA_0 are assumed. Setting the latter to zero would practically cut the bubble amplitudes at later times by two.

As indicated above, the relation (4.3) will be used until a time t_1 in which the bubble speed A equals the terminal bubble speed $\dot{A}_t$:

$$\dot{A}(t_1) = n A_0 e^{n t_1} = \dot{A}_t$$

which gives $$A_0 = \dot{A}_t \cdot \frac{1}{n} e^{-n t_1} \quad , \tag{4.4}$$

and $$A(t_1) = A_0 e^{n t_1} = \frac{1}{n} \dot{A}_t \quad , \tag{4.5}$$

and $$t_1 = \frac{1}{n} \ln \left(\frac{\dot{A}_t}{n A_0} \right) \quad . \tag{4.6}$$

The terminal bubble speed $\dot{A}_t$ is given by

$$\dot{A}_t = F \cdot (g \lambda)^{1/2} \tag{4.7}$$

where λ is the wavelength, g the acceleration, and F an empirical constant which is often called the Froude number. This constant has been determined experimentally to lie in the range 0.2 ... 0.3 by Emmons, Chang, and Watson (1960), theoretical considerations placed it at about 0.24, Garabedian (1957), or between 0.22 and 0.24, Birkhoff and Carter (1957). Purely numerical simulation by Harlow and Welch (1966) gave results in agreement with Garabedian (1957). Using other numerical techniques, Baker, Meiron, and Orszag (1980) found F = 0.225± 0.002 (after an extrapolation) and Menikoff and Zemach (1983) found F = 0.23. The only fully analytical determination is due to Layzer (1955) or Kull (1983) (see paragraph 4.3) and gives

$$F = (6\pi)^{-1/2} \approx 0.230 \tag{4.8}$$

in good agreement with the other results. This value of F will be used in what follows. (See, however, the discussion in 5.4.4.)

In summary, bubble growth is described by the following equations:

$$A(t) = A_0 e^{nt} \qquad \text{for } t \leq t_1 \tag{4.9}$$

$$A(t) = \frac{1}{n} \dot{A}_t + \dot{A}_t (t - t_1) \qquad \text{for } t \geq t_1 \tag{4.10}$$

where $\dot{A}_t$ is given by (4.7) and (4.8) and t_1 is defined by (4.6).

Introducing the non-dimensional quantities

$$\alpha = A k \tag{4.11}$$

and

$$\tau = t (g k)^{1/2}, \tag{4.12}$$

the above relations read:

$$\alpha(\tau) = \alpha_0 \, e^{n(gk)^{-1/2}\tau} \qquad \text{for } \tau \leq \tau_1 \qquad (4.13)$$

$$\alpha(\tau) = \frac{(gk)^{1/2}}{n} \dot{\alpha}_t + \dot{\alpha}_t (\tau - \tau_1) \qquad (4.14)$$

$$\text{for} \quad \tau \geq \tau_1$$

$$\text{where} \quad \dot{\alpha}_t = (3)^{-1/2} \qquad (4.15)$$

$$\tau_1 = \frac{(gk)^{1/2}}{n} \ln\left(\dot{\alpha}_t \frac{(gk)^{1/2}}{n \alpha_0}\right), \qquad (4.16)$$

and the dot, when used in connection with dimensionless variables, denotes derivation with respect to τ.

Here it should be noted that

$$n/(gk)^{1/2} = y^{1/2} \qquad (4.17)$$

after (2.14). An illustration of the model for the classical case y = 1 will be given in Figures 10 and 11.

Similar models have been developed independently by Frieman (1954), Layzer (1955), Fishburn (1974), Suydam (1978), and Pilch et al. (1981). The model presented here very much resembles the one due to Layzer (1955). In all these models, the growth constant n contained in (4.9) and (4.10) has been determined from the classical formula (2.21) together with (2.14). This would not be appropriate in the presence of a gradual density transition which, as discussed in the previous chapter, can effectively reduce the growth constant. For the linear phase this can be accounted for by determining the growth constant n from (2.14) and (3.1). Unfortunately, there is no relation available describing the effect of the density gradient on

the terminal bubble speed. So, one cannot take advantage of this possibly important effect and the analysis of bubble growth is inconsistent with this respect. Strictly speaking, there is even no evidence available, which indicates that the nonlinear behaviour at really gradual density transitions corresponds to that observed at density steps with large Atwood ratios. It is, however, expected (and assumed in the synthetical model) that the latter constitutes an upper limit to instability growth in the nonlinear regime as it does in the linear regime.

The model presented here assumes the Atwood ratio A to be close to one. A generalization to smaller values of A is easy for the linear part of the model only. It would consist of replacing the simple formula (3.1) by the equations (2.40) and (2.41). Guidance in deciding whether the extra expenditure were worthwhile could be obtained from Figure 4. The situation is not as clear for the nonlinear phase. First, even for density jumps the physical picture outlined in section 4.1 is valid for large Atwood ratios, above 0.5 say, only. Second, it is not clear whether the terminal bubble speed depends on the Atwood ratio. Birkhoff (1955), using approximate arguments, derived that the terminal bubble speed would vary as $\sqrt{1-\varrho_1/\varrho_2}$. However, Daly (1966) as well as Crowley (1970) found no dependence of the terminal bubble speed on the Atwood ratio in the range $0.33 \leq A \leq 0.82$ in their numerical simulations using the MAC method. It is hoped that a generalization of the nonlinear theory to be presented next can remove this discrepancy.

The criterion used in this model for switching from the linear theory to the terminal bubble speed may also be taken as an indication of the range in which linear theory can be applied reasonably. It is, therefore, interesting to note that the criterion which has been formulated using the growth velocity can be translated into one which is based on the amplitude. From

$$\dot{A}(t_1) = \dot{A}_t^{\circ} \tag{4.18}$$

one obtains

$$A(t_1) = \frac{1}{n} \dot{A}_t^{\circ} \tag{4.19}$$

either on the basis of assumption (4.2) or assuming t_1 to be so large that $\exp(-nt_1)$ may be neglected, i.e. assuming a very small A_0. With

$$n = \sqrt{ygk} \tag{4.20}$$

after (2.14) and (4.7) this gives

$$A(t_1) = \frac{F \cdot \lambda}{\sqrt{2\pi y}} \tag{4.21}$$

which becomes

$$A(t_1) = \frac{\lambda}{2\pi\sqrt{3y}} = \frac{1}{\sqrt{3y}\,k} \tag{4.22}$$

after (4.8). In the classical case of an interface, y = 1 and

$$A(t_1) = \frac{\lambda}{2\pi\sqrt{3}} = \frac{1}{\sqrt{3}\,k} \tag{4.23}$$

which is a little bit larger than the value $\lambda/6\pi$ given by Kull (1983) but still much smaller than the value of $0.4\,\lambda$ which is often cited as the amplitude at which nonlinear behaviour starts.

In the presence of a gradual density transition, y will be smaller than one and the amplitude range in which linear theory is applied will be extended.

It should be mentioned that these results are obtained only if one assumes (4.2) or small initial amplitudes. In general, the switch-over amplitude obtained from the velocity criterion will depend on the initial amplitude.

4.3 Nonlinear theory of bubble growth

Layzer (1955) has developed a nonlinear theory describing the motion of the bubble vertex. Kull (1983) within a more complete study of nonlinear bubble growth has repeated the derivation allowing for an initial velocity disturbance. The result is an analytical formula giving the bubble speed $\dot{\alpha}$ as a function of the initial conditions α_0 and $\dot{\alpha}_0$ and the actual bubble amplitude α:

$$\dot{\alpha}^2 = \frac{\frac{2}{3}\left[1 - e^{-3(\alpha-\alpha_0)}\right] - e^{-3\alpha}\left[2(\alpha-\alpha_0) - \dot{\alpha}^2(1+2e^{3\alpha_0})\right]}{2 + e^{-3\alpha}} \quad (4.24)$$

Numerical integration of (4.24) gives the nonlinear development of the bubble amplitude in full agreement with all available information. In particular, as pointed out by Kull (1983), for small amplitudes, $3\alpha \ll 1$, one obtains (in nondimensional form) the result (2.12) known from linear theory and in the limit of large amplitudes, (4.24) reduces to (4.15) which is the nondimensional equivalent of (4.7) and (4.8).

As a first application, the synthetical model presented in the last section is compared with pure linear theory and the fully nonlinear theory in Figures 10 and 11. To this end, equations (4.13) to (4.16) are applied to the classical case of superposed fluids with an Atwood ratio of one, in which case

$$n = (gk)^{1/2} . \quad (4.19)$$

Furthermore, as a typical initial condition,

$$\alpha_0 = \dot{\alpha}_0 = 0.01 \quad (4.20)$$

is chosen. Figure 10 showing the (logarithm of the) bubble growth rate is the equivalent of Fig. 6.1 in the report by Pilch et al. (1981) but is no longer based on physical intuition only. Figure 11 which shows bubble amplitudes demonstrates that the empirical model overestimates the amplitude because it overestimates the growth rate during the transition regime between the true linear regime and the asymptotic nonlinear regime. It furthermore demonstrates the potential big advantage of the synthetical model over linear theory. (In a similar figure by Layzer (1955) obviously

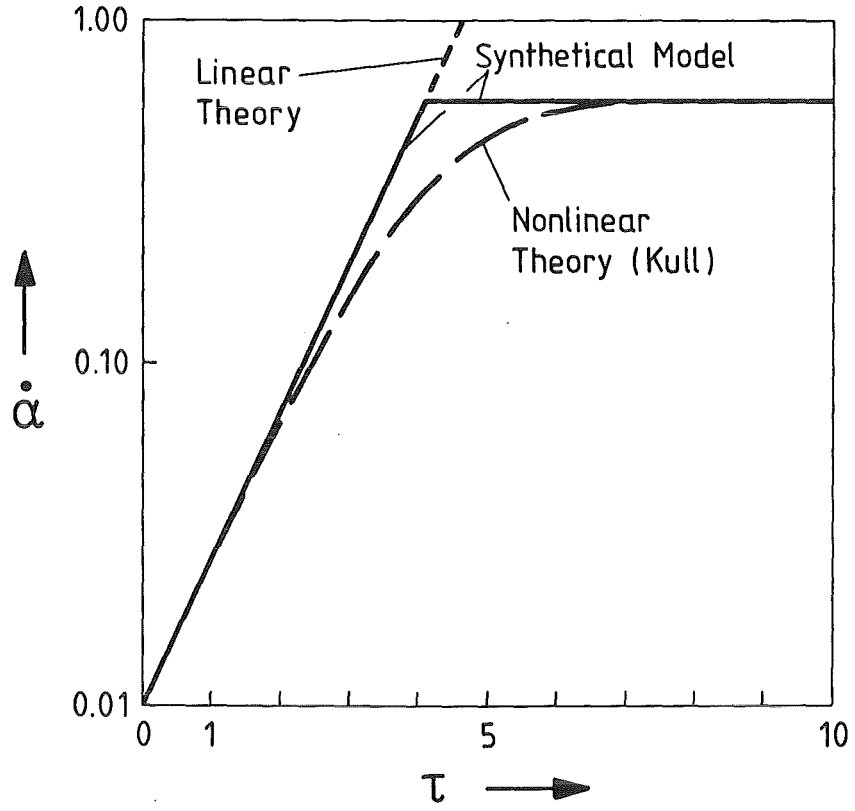

Figure 10: Comparison of bubble growth rates

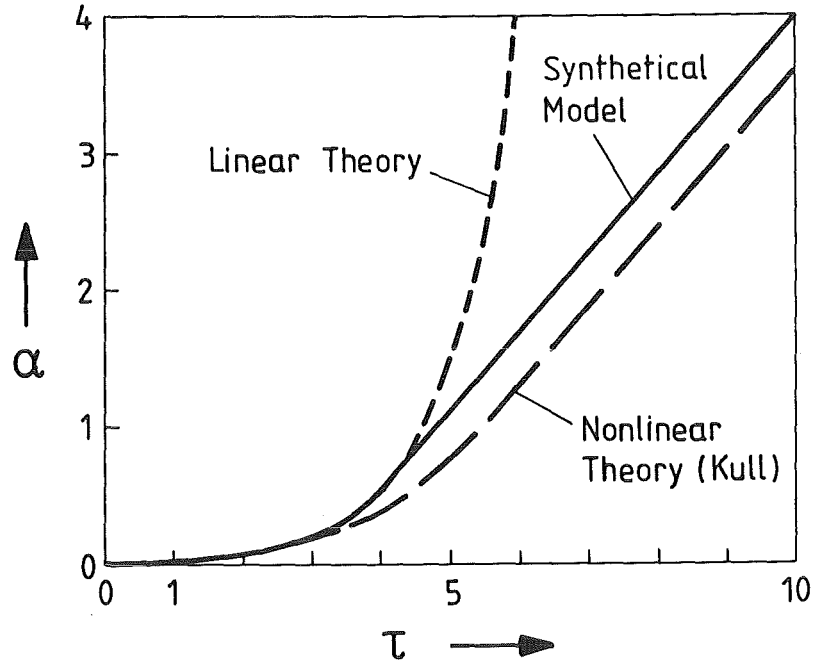

Figure 11: Comparison of bubble amplitudes

the curve labels have been exchanged by mistake: a should read B, A should read b, and vice versa.)

The nonlinear theory by Layzer (1955) has been extended to include surface tension by Rajappa (1967). From this, in particular, the effect of surface tension on the terminal bubble speed may be obtained which, however, is not considered here.

4.4 Other nonlinear theories

Since linear theory becomes increasingly doubtful as the amplitude grows, there have been many attempts to develop higher-order theories, mainly for the "classical" situation of two-dimensional disturbances at the interface between a semi-infinite fluid and vacuum. Probably the first to do so was Ingraham (1953) who presented the principle equations and worked out the second-order solution. His theory was generalized by Baker and Freeman (1981) to include initial velocity disturbances.

Emmons, Chang, and Watson (1960) developed a third-order theory including surface tension in order to study finite initial amplitude effects on the stability criterion, i.e. on the critical wavenumber beyond which instability is prevented by surface tension. But as discussed e.g. by Kiang (1969) and Rajappa (1970) their method was inappropriate and partially gave wrong results. Later the destabilizing effect of finite initial amplitudes (the critical wavenumber increases with initial amplitude) has correctly been derived by Kiang (1969), Nayfeh (1969) and Amaranath (1980). Nayfeh also gave a second-order solution for the unstable case, remarking correctly that it is valid only for short times. (Nayfeh in addition studied the effect of a finite thickness of a fluid layer which is bounded by a flat plate).

Rajappa (1970a, 1970b) presented a third-order theory including surface tension. While his result on the critical wavenumber is incorrect (see Nayfeh or Amaranath) he presents (in the second paper) results indicating that his theory is able to describe the development of instabilities well into the nonlinear regime with a steadily growing bubble. Amaranath and Rajappa (1976) have extended the theory to include a finite density of the

lighter fluid and Rajappa and Amaranath (1977) have studied three-dimensional disturbances (presenting only second-order results for the amplitude).

The difficulty with all the higher-order theories for unstable cases is to find out how far in time they can be used. It is clear that they must fail at some time because the higher-order terms (i.e. higher terms in a Fourier series) are kept small by increasing powers of the initial amplitude h_0 only, i.e. they are proportional to h_0, h_0^2, h_0^3, etc. On the other hand their time behaviour is characterized by exp(nt), exp(2nt), exp(3nt), etc. so that inevitably, after some time, higher-order terms will become more important than terms of lower order, indicating bad convergence of the series, the first two or three terms of which are considered only. The above considerations also indicate that decreasing the growth constant n increases the time interval in which any finite-order theory may be applied. In the case of linear theory and assuming the switch-over criterion of the synthetical model of subsection 4.2 even the amplitude up to which it could be used was increased by decreasing n (see the end of section 4.2). Hence, with a strong influence of surface tension, third-order theory may accurately describe the disturbance amplitudes up into the nonlinear regime as presented in Figures 2 and 3 of Rajappa (1970b). But it seems difficult to predict e.g. the terminal bubble speed from such a theory and without additional information (as e.g. an experiment) because it is completely unknown (within the theory) whether the terminal bubble speed is reached at all within the range of validity of the theory, and if it were, at what time.

Without surface tension, the above theories are of rather limited use for a description of the disturbance amplitudes because the higher-order Fourier terms, as indicated above, grow with higher powers of exp(nt), Therefore, the period in which they are already large enough to really contribute to the sum of the series but still smaller (by an order of magnitude, say) than the preceding term is rather limited. An illustration of this for the second-order term is given in Figure 7 of Prosperetti and Jacobs (1983). (By the way, their somewhat higher estimate of the Froude number characterizing the terminal bubble speed may be due to the fact that their method gives a bubble which is slightly peaked at the top.) The numerical results represented in that figure also show that for any term

the period until the next higher term becomes important too becomes rapidly smaller with the order of the term. In other words, the number of terms required for a reasonable description of the interface increases rapidly and at an increasing rate. Therefore, adding higher-order terms becomes increasingly inefficient (and, in addition, much more involved).

A completely different approach to a nonlinear theory of Rayleigh-Taylor instability is the generalized coordinate method developed by Dienes (1978). This method is quite promising because it rather elegantly describes the shape variation of the interface and (when an ordinary differential equation is integrated numerically) allows for considerable freedom in including real fluid effects (but not compressibility). However, as presented in the paper, i.e. with only one term retained in the series expansion of the velocity field (only one generalized coordiante), it gives absurd late-time results: the spike amplitude becomes infinite within a finite time while the bubble amplitude remains below a fixed value.

5. Applications to pusher shell breakup

5.1 Formulation of the problem

As already described in the introduction, inertial confinement fusion requires extremely high fuel densities and during the implosion which shall lead to them, Rayleigh-Taylor instabilities can occur because pusher material at low density but high temperature and therefore high pressure is accelerating compressed but much colder pusher material (and the fuel in front of it). The instability zone which e.g. in Figure 1b is located roughly between 2.66 mm and 2.77 mm is characterized by a gradual density transition. It is essential that the thin shell of compressed pusher material in front of it is not broken up by the instabilities, i.e. not penetrated completely by the "bubbles" filled with light and hot material. Numerical pellet simulations performed under the assumption of spherical symmetry do not answer this question directly. Two-dimensional pellet simulations, even if available, are very involved. Therefore, a separate model is needed. Here, the synthetical model presented in the last chapter is used to determine maximum allowable initial perturbations which can serve as figure of merit when comparing different pellet designs and/or illumination histories with respect to the pellet's vulnerability to pusher shell breakup on the basis of information provided by spherical pellet simulations.

For two reasons the allowable initial amplitude characterizing both initial perturbations cannot simply be compared directly with some other figure to decide whether the pusher shell in a certain case should survive. Firstly, the model is overly pessimistic. Although it accounts for two important effects, the gradual density transition and the nonlinear growth saturation, it leaves out many other effects that might further strongly reduce instability growth, as e.g. lateral heat transfer. It is difficult to judge how important such effects are without having tested them under the appropriate boundary conditions. For example, in all studies on laser fusion the density gradient is so steep that it has little effect on instability growth, while, in the present case it well makes a difference, as will become obvious soon. There are, of course, also effects that can increase the growth rate. But their potential seems not to be too great. They will be discussed in some more detail in a separate section of this chapter. The second obstacle preventing direct

comparison of the maximum allowable initial perturbations with the actual initial perturbations is absence of information on the latter. In the literature, the discussion concentrates on surface imperfections and for reasons that are far from being clear, surface imperfections below 10 nm are quoted as necessary and possible (e.g. Bangerter and Meeker (1977), Hendricks et al. (1981)). This figure, however, may be rather meaningless in the present context, since, as e.g. in the here considered illustrating case, the instability under discussion may not grow at a material interface but at a density gradient that develops within the pusher material. One could imagine that distortions develop in this region during the acceleration process because imperfections of the pusher-fuel interface imply variations of the (areal) mass to be accelerated. Initial perturbations so produced may be characterized as kinematic in contrast with static prefabricated perturbations. They have been observed by Ripin et al. (1982). Such disturbances will always grow because of both effects: kinematics and Rayleigh-Taylor instability. In the beginning, kinematics will prevail, but later instability growth may predominate. (The above mentioned experiment seems not to have entered the second stage.) In this situation it is difficult to determine an initial amplitude. Most probably, however, both, initial amplitude and initial (disturbance growth) velocity must be taken to be nonzero. Therefore, the assumption (4.2) has been chosen for the synthetical model.

Application of the synthetical model in conjunction with the estimate of instability growth at gradual density transitions presented in chapter 3 means that the linear growth constant is calculated for a region of exponentially increasing density between regions of constant densities (see Figure 7b) and a constant acceleration in the positive z-direction. In order to specify a breakup criterion it is observed that the pusher shell assumes a minimum thickness d during the compression phase and rapidly grows thicker afterwards due to spherical convergence. The shell is assumed to remain intact as long as the bubble amplitudes do not become larger than the minimum thickness d. In addition, for the following numerical example, the wavelength is assumed to equal the minimum thickness d, too, because it is common practice to assume this wavelength to be most dangerous. The most dangerous wavelength will be discussed in more detail in the third section of this chapter.

5.2 Determination of maximum allowable initial perturbations

5.2.1 Numerical example

Tahir and Long (1982) have simulated the performance of a former HIBALL pellet with the MEDUSA code and provided the information necessary to apply the synthetical model. This case has already been studied with a similar model by Jacobs (1983). But that study still used the result of the theory by LeLevier et al. (1955), which now has been shown to be wrong. Therefore, the case is reconsidered here.

As determined by Tahir and Long (1982), the Atwood ratio formed with the two extreme densities is close to one all the time, the minimum thickness is

$$d = 16\,\mu m\,, \tag{5.1}$$

the total acceleration time is,

$$t_2 = 8\ ns\,, \tag{5.2}$$

the acceleration gives

$$g = 2.5 \cdot 10^{13}\ m/s^2 \tag{5.3}$$

and the inverse length scale of the density gradient is

$$\frac{1}{L} = \beta k = 7.39 \cdot 10^{4}\ m^{-1} \tag{5.4}$$

so that with

$$\lambda = d = 16\,\mu m \tag{5.5}$$

$$k = 3.93 \cdot 10^{5}\ m^{-1} \tag{5.6}$$

and

$$\beta = 0.188\,. \tag{5.7}$$

From (5.3) together with (4.7) and (4.8) one gets

$$\dot{A}_t = 4\,600 \text{ m/s}.$$

Now, after (4.10)

$$A(t_2) = \frac{\dot{A}_t}{n} + \dot{A}_t (t_2 - t_1)$$

so that $$t_1 = \frac{1}{n} - \frac{A(t_2)}{\dot{A}_t} + t_2 \quad . \tag{5.8}$$

Here, after (2.14)

$$n = (\gamma g k)^{1/2} \tag{5.9}$$

where y is replaced by y* after (3.1) since $\beta < 0.5$ and $A \gtrsim 0.95$:

$$\gamma \lesssim \gamma^* = \frac{\beta}{1 + \beta^2/4} \approx 0.186 \; . \tag{5.10}$$

This value shows that the gradual density variation, in this case, reduces the growth constant by a factor

$$(0.186)^{-1/2} \approx 2.3$$

as compared to the classical value given by y = 1. From (5.9)

$$n = 1.353 \cdot 10^9 \text{ s}^{-1} \tag{5.11}$$

and with this and (5.8) $$t_1 = 5.261 \text{ ns} \tag{5.12}$$

so that, after (4.4)

$$A_0 = 2.75 \text{ nm} \tag{5.13}$$

which implies, after (4.2),

$$\dot{A}_0 = n A_0 = 3.73 \text{ m/s} \; . \tag{5.14}$$

These are the amplitudes of the maximum allowable initial perturbations.

Growth of the here discussed disturbance with these initial conditions is shown in Figure 12, comparing linear theory and the synthetical model, which both take into account the retarding effect of the gradual density transition, and the nonlinear theory of Kull, in which this effect cannot be accounted for. Actually, consistent use of (4.2) leads to different initial velocity disturbances, the one used in connection with Kull's theory being larger. But use of the same initial velocity shifts the straight part of the curve to the right by 0.1 ns only. So this effect may be neglected.

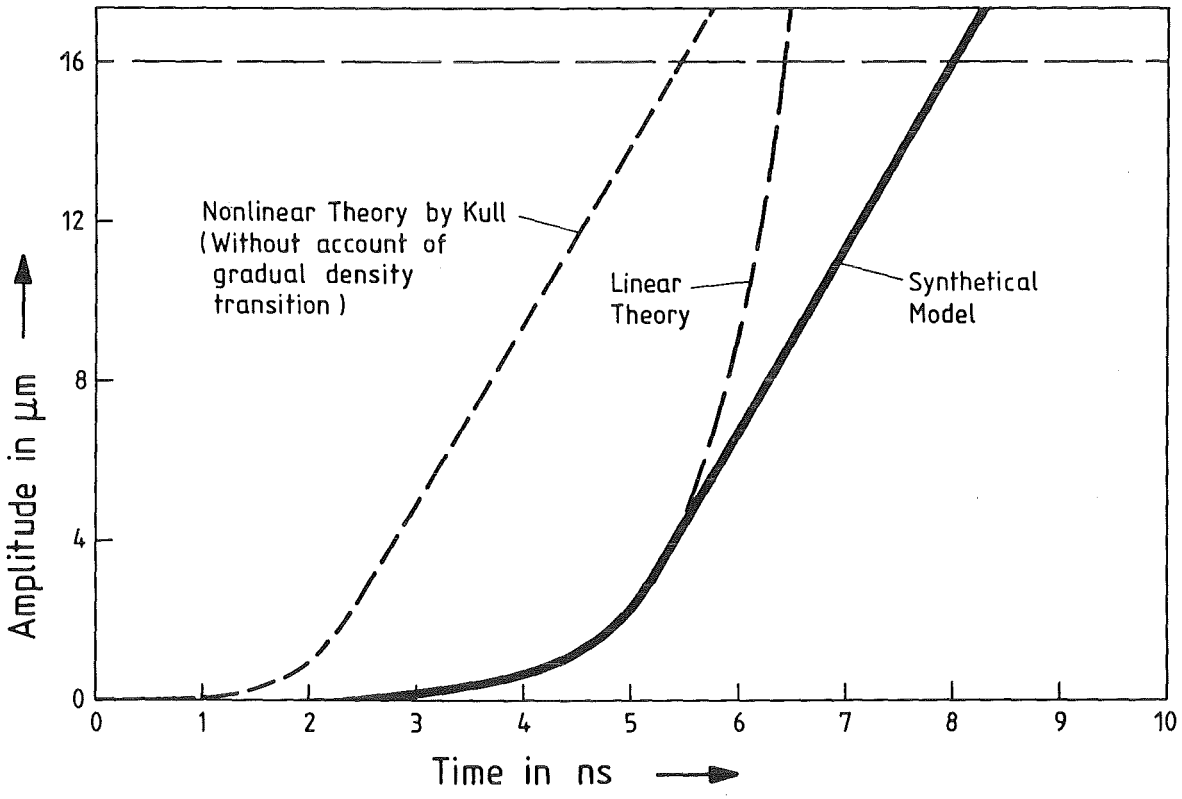

Figure 12: Growth of bubble amplitude in the HIBALL pellet case, assuming the maximum allowable initial perturbation amplitudes after (5.13) and (5.14). Comparison of empirical model, linear theory and nonlinear theory due to Kull (1983).

The above determined allowable initial displacement amplitude is an extremely small fraction of the wavelength ($2 \cdot 10^{-4}$). Therefore, initial amplitudes even ten times as large are still in the range where linear theory applies and the synthetical model as formulated here always overestimates the bubble growth velocity. So, with initial amplitudes that allow survival of the pusher shell, this model will always be conservative.

In order to further illustrate the importance of the two effects which are included in the synthetical model one may calculate the figure of merit, A_0, with linear theory alone and/or the growth constant $n = \sqrt{gk}$ appropriate for a free surface (A = 1 being assumed throughout). The results are as follows:

Full synthetical model:	$A_0 = 2.75 \cdot 10^{-9}$ m
Linear theory with account of gradual density transition:	$A_0 = 0.32 \cdot 10^{-9}$ m
Synthetical model without account of gradual density transition:	$A_0 = 0.2 \cdot 10^{-12}$ m
Linear theory without account of gradual density transition:	$A_0 = 0.2 \cdot 10^{-15}$ m

The last two numbers which are small even on atomic and nuclear length scales, respectively, show how important it is to account for effects that reduce the linear growth constant like (in this case) the gradual density transition. They also show that nonlinear saturation becomes more important with increasing linear growth constant. But even in the case studied here with its small growth constant, nonlinear saturation still contributes one order of magnitude.

5.2.2 Possible extensions

In the example presented in the last subsection the result partially depends on the procedure by which the parameters (boundary conditions) are

determined from the numerical pellet simulation. So, the above presented result is not necessarily as conservative as the synthetical model is. For instance, as can be seen from Figure 1b, the density profile in the case considered is far from being exponential. In that case it would be conservative to define β as the spatial maximum of the logarithmic derivative of the density distribution. Actually, the β used above is some spatial mean value defined by

$$\beta = \frac{1}{\Delta} \ln \frac{\varrho_2}{\varrho_1} \tag{5.15}$$

where Δ is the (dimensionless) thickness of the transition region taken to be bounded by z_1 and z_2, i.e.

$$\Delta = k (z_2 - z_1)$$

and

$$\varrho_2 = \varrho(z_2)$$

$$\varrho_1 = \varrho(z_1).$$

On the other hand, the β used in the numerical example is the largest that has been found during the whole acceleration phase and represents a rather sharp maximum. Before and after this maximum, β is only about half as big. Therefore, the β used should still be conservative. Similar considerations apply to the acceleration which, however, seems to vary less with space and time.

A more elegant and more realistic way to treat the problem would be to take the actual density profile. For the period in which linear theory applies, this can be achieved using a formalism developed by Mikaelian (1982). He has derived formulas to calculate the fastest growing instability mode of an arbitrary density profile given as a series of density steps. This is just as the finite-difference pellet simulation codes determine the density profile. With this method the largest growth constant could be determined directly and without recourse to an exponentially varying density and the corresponding analytical relations used in this report.

Of course, the determination of the largest growth constant may be repeated after certain time intervals (not necessarily after each time step). At the same times the (spatial maximum of the) acceleration may be determined and both data may be used to calculate instability growth with almost full time dependence. This procedure would remove avoidable pessimism and the necessity to define an acceleration time interval.

The above outlined scheme in which instability growth is calculated in several time steps could probably be extended to account for another effect which may be expected to reduce instability growth: convection or flow of material through the instability zone. In the present context where only an acceleration which is constant in space can be considered, the instability zone is identical with the density transition region and convection will occur if the region of increasing density moves forward (in the direction of the acceleration) with respect to the Lagrangian mesh cells. Since the disturbance amplitude quickly dies away with distance from the location of maximum disturbance, this convection of formerly further away material layers into the zone of increased disturbance growth (the density transition zone and possibly its close vicinity) would continuously reduce the initial amplitudes to be considered in the next time step. While this growth reducing effect occurs where it is needed - upstream, i.e. towards the pusher shell - disturbance amplitudes will be increased downstream where they do not matter. How important this effect might be remains to be clarified.

Clearly, this concept requires calculation of the z-dependence of the disturbances. But that can be done straightforward as demonstrated in chapter 2 (see Figure 2) for continuous density variations and by Mikaelian (1982, 1983a,b) for multiple step functions. It is further necessary that the maximum growth constant is used only in connection with that portion of the initial amplitude at a certain location which is the component of that amplitude corresponding to the fastest growing eigenmode. The same fact is expressed by Mikaelian (1983a) slightly different: In order that the disturbance everywhere grows as a normal mode (i.e. with one growth constant) the initial disturbances have to be proportional to the corresponding eigenfunction. But, of course, additional amplitudes may be present - they just do not grow so fast. If, e.g. the here outlined scheme is coupled with a calculation of the kinematic development of

initial disturbances as discussed in subsection 5.1.1, the initial disturbances will be equal at all interfaces. But only at the location of the maximum of the eigenfunction this whole initial disturbance will be considered as initial value. At other locations the effective initial amplitudes will be smaller corresponding to the shape of the eigenfunction.

In the discussion so far it has been assumed that instability growth can effectively be described by the fastest growing instability mode only. Actually it might be necessary to take into account several modes - but probably a few are enough. This is no principal difficulty but only increases the numerical effort. The problem has been treated by Mikaelian (1983a,b).

The time dependent method discussed here can also be made to account for another effect which - again - has already been mentioned by Mikaelian (1984): If the material is compressed during the acceleration or if it expands at some other time, always the disturbance amplitudes are reduced or increased correspondingly. This is another effect modifying the z-dependence of the disturbance amplitudes. If it is taken into account also, it might really be necessary (or at least prudent) to decompose at any time step the actual z-distribution of the amplitudes into the components corresponding to the (most important) eigenfunctions of the new density profile. Of course, compression or extension of existing disturbance amplitudes is only part of the effect that material compressibility has. While, in the present context, collision of shells as mentioned by Mikaelian (1984) is of no concern, one has to worry about the increasing effect which compressibility may have on the growth constants. This effect will be discussed in a further section of this chapter.

The discussion of the extended calculational scheme so far was limited to the linear phase. Nothing nearly as sophisticated is available for the nonlinear phase. The best (i.e. least conservative) is to assume the terminal bubble speed given by (4.7) and (4.8) to take over when the growth rate of the disturbance at the rear interface of the pusher shell reaches this velocity. This proposal makes use of the fact that disturbances grow the fastest somewhere in the middle of the density transition region. So the terminal bubble speed will be reached there earlier. However, there is no easy way to calculate individual disturbance amplitudes at the different

interfaces after switching to the terminal bubble speed because the z-dependence of the corresponding flow field is difficult to determine. One only knows that higher harmonics couple in with increasing weight. But elongated use of linear theory is conservative because the disturbance amplitudes in the middle of the density transition region (which, however, are of no direct concern) will be overestimated and because the fundamental mode considered in linear theory dies out slower in the z-direction (essentially as exp(-kz)) than the higher modes which actually will come into play, and which die out faster, e.g. as exp(-2kz) and exp(-3kz).

5.3 Most dangerous wavelength

5.3.1 Introductory discussion

Since the synthetical model presented in paragraph 4.2 describes the growth of disturbances basically correct up to the range in which destruction of the pusher shell occurs, this model is suited to determine the most dangerous wavelength. There are two ways to do so: The first consists of determining the breakthrough time at which the bubble reaches a certain amplitude (in the following called critical amplitude). The most dangerous wavelength then is the one with the shortest breakthrough time. (Just as well one might determine the wavelength reaching the largest bubble amplitude within a certain time interval.) This procedure has the disadvantage that the result not only depends on the critical amplitude chosen but also on the assumed initial disturbances, and that the breakthrough time is a rather insensitive parameter. On the other hand, it has the advantage that it can be used when the time variation of the density gradient and the acceleration shall be accounted for. Also, this procedure has already been used by Frieman (1954), Capriotti (1973), Fishburn (1974), Suydam (1978), and Jacobs (1983). It is therefore again considered here to some extent in order to demonstrate it in conjunction with the revised synthetical model.

The second possibility for determining a most dangerous wavelength is to calculate the maximum allowable initial perturbations as a function of the wavelength and looking for the minimum of this curve. While this procedure can be followed only if the density gradient and the acceleration are assumed constant in time, one need not assume initial perturbations and the results are more pronounced because the maximum allowable initial

perturbations are a much more sensitive parameter - making it a suitable figure of merit.

In a further subsection the potential effect of a reduction of the terminal bubble speed by gradual density transitions is explored by assuming a corresponding relation.

5.3.2 Determination from shortest breakthrough time

Inverting (4.10) and inserting (4.6) one obtains

$$t_2 = \frac{A^*}{\dot{A}_t} + \frac{1}{n}\left[\ln\left(\dot{A}_t/nA_0\right) - 1\right] \qquad (5.15)$$

as the breakthrough time, i.e. the time to reach a critical amplitude which is here called A*. This formula is valid as long as A* is larger than the switch-over amplitude $A(t_1)$ which is $\left[\sqrt{3y}\,k\right]^{-1}$ after (4.22). Thus, for the example treated in the last paragraph, i.e. A* = d = 16μm and a length scale of the density variation of $L = 1/\beta k$ = 13.53 μm, (5.15) is valid up to the wavelength λ = 174 μm, in which case β is just larger than 2 so that already 1 is the conservative approximation for y. The result is shown in Figure 13 for different choices of the parameters n and A_0. All the curves show minima (which have been marked) because disturbances with shorter wavelengths have larger growth constants in the linear phase but reach the nonlinear phase earlier and then grow at a slower rate while disturbances with longer wavelengths have smaller growth constants in the linear phase but grow faster in the nonlinear phase. The most dangerous wavelength λ^* depends slightly on the initial disturbances. Figure 13 shows however that it is larger than the critical amplitude A* in all the cases considered here. It also shows that the curves are very flat around the minima.

When calculating the curves A, B, and C the density gradient has been taken into account by using a growth constant n determined with y = y* after (3.1). A certain density gradient (with fixed length scale L) slows down shorter wavelength disturbances more efficiently than those with

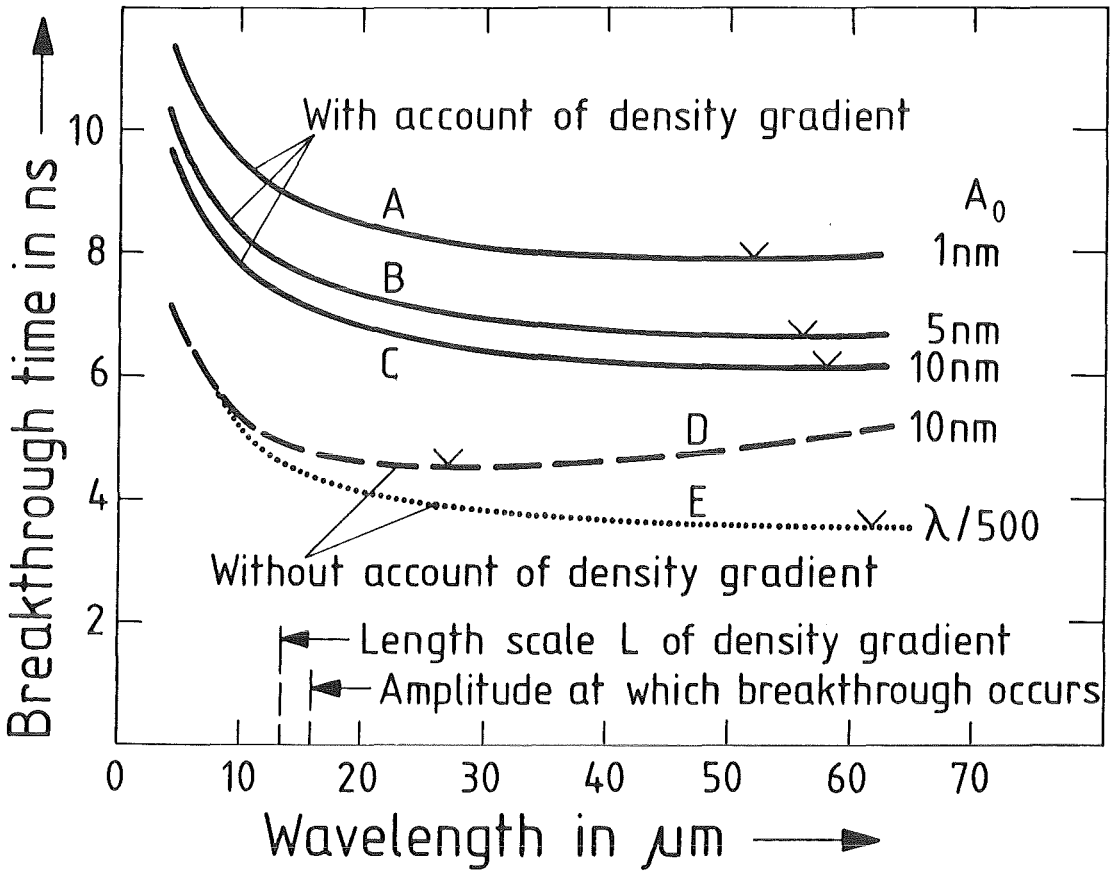

Figure 13: Breakthrough time as a function of wavelength and initial disturbances (A_0 as indicated, $\mathring{A}_0 = nA_0$)

larger wavelengths. This is not only true for the linear phase where it is accounted for in the present model but also in the nonlinear phase (if a density gradient reduces the terminal bubble speed). Therefore, at a gradual density transition, the most dangerous wavelength is larger than at a density step. This is demonstrated by curves C and D which use the same initial displacement amplitude. But curve D has been obtained using the classical growth constant for density steps with y = 1. Curve D has

its minimum at about 1.7 times the critical amplitude A*, while the minimum of curve C lies at 3.6A*. If the gradual density transition would really reduce the ultimate bubble speed, the most dangerous wavelength would become even larger. Therefore, the most dangerous wavelength at a gradual density transition may be expected around 4A* if the initial disturbances of all wavelengths are equal and it may lie between 2A* and 8A* depending on which wavelength has the largest initial disturbances if those are randomly distributed.

Finally, curve E in comparison with curve D shows that even for a density step the most dangerous wavelength occurs at much higher values if the initial displacement amplitude is assumed proportional to the wavelength. This may explain why Kull (1982) with his simplified nonlinear model of bubble growth also finds rather large ratios between most dangerous wavelength (in his case the wavelength reaching the highest bubble amplitude within a certain time) and critical amplitude (in his case the maximum bubble amplitude) as illustrated in his Figure 4. Actually, use of the assumption (4.2) in all the cases presented means that the initial velocities decrease with growing wavelength (or increase only with $\sqrt{\lambda}$ instead of λ for curve E). This tends to give smaller most dangerous wavelengths here and in the next subsection.

5.3.3 Determination from smallest maximum allowable initial disturbances

In this case just the procedure followed in subsection 5.1.2 is conducted for different wavelengths λ. The result, still for the same example, is shown as curve A in Figure 14. While the most dangerous wavelength (52 μm) is in the range expected after Figure 13, Figure 14 shows also that the maximum allowable initial disturbances at this most dangerous wavelength are much smaller than those obtained for λ = 16 μm, an effect which is not so clearly indicated by Figure 13. Of course, if one wanted to determine whether a fusion pellet will work, the smallest maximum allowable initial disturbances would be those which had to be compared to the unavoidable initial perturbations. The corresponding initial displacement amplitude A_0 is therefore called the critical initial amplitude A_0^*. The range of wavelengths to be considered for this purpose would still be rather large (e.g. 2A* to 5A*) because also the here obtained curve is flat around the

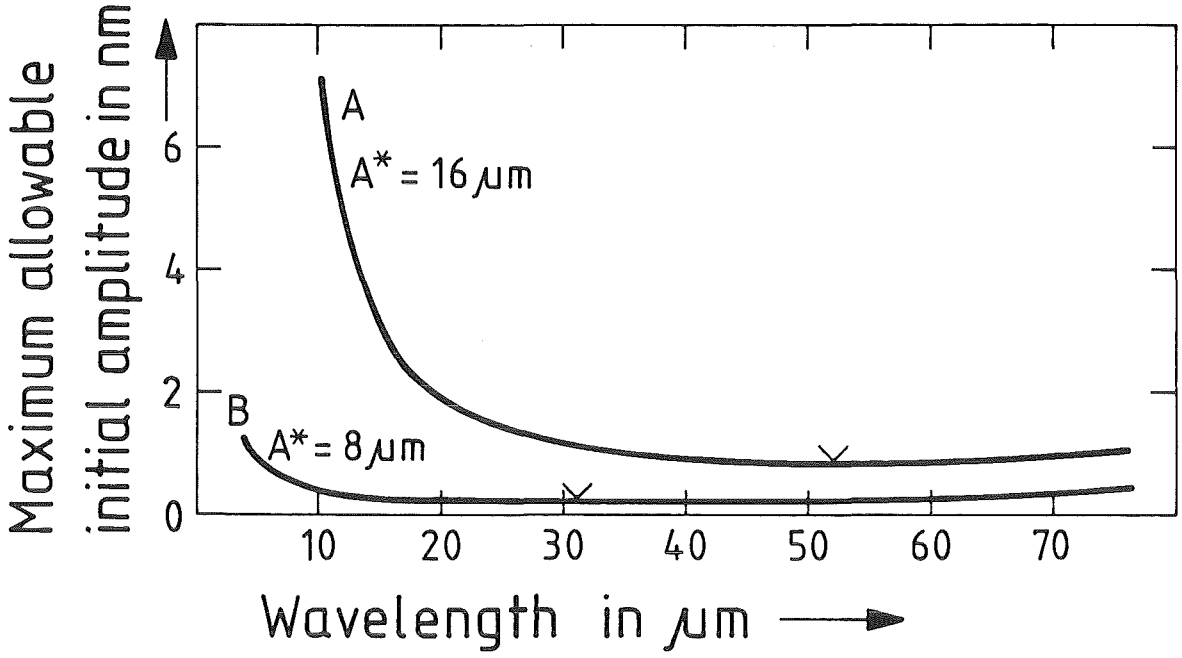

Figure 14: Maximum allowable initial amplitude A_0 which implies an initial velocity $\dot{A}_0 = nA_0$ as a function of wavelength and initial disturbances.

minimum. In this context it is important to note how strongly the critical initial amplitude depends on the critical amplitude A*. The critical initial amplitudes obtained for A* = 16 µm, 8 µm, and 5 µm are 0.88 nm, 0.21 nm, and 0.11 nm, respectively (see also curve B in Figure 14). A thicker minimum shell thickness d which means a larger critical amplitude A*, therefore, has an important effect on the critical initial amplitude A_0^*. Hence, to design a pellet which is resistent against pusher shell breakup by Rayleigh-Taylor instabilities is much easier for a breakeven experiment than it is for a pellet with a gain appropriate for a fusion reactor. For in the second case the necessary high hydrodynamic efficiency of the compression process requires a small minimum pusher shell thickness.

Curve B in Figure 14 also shows that the most dangerous wavelength λ^* is roughly proportional to the critical amplitude A*. The ratios of λ^*/A^* obtained for A* = 16 μm, 8 μm, and 5 μm are 3.3, 3.9, and 4.0, respectively. Therefore, when comparing different pellet simulations, it is reasonable to assume λ in each case to be 3 or 4 times the critical amplitude which, in turn, is some fraction of the minimum pusher shell thickness (e.g. A* = d) observed in the different cases. In addition, curve B in Figure 14 shows that the range of potentially dangerous wavelengths has increased with decreasing A*. For A* = 8 μm it extends from A* to 10 A*, roughly.

If the "classical" growth constant appropriate for a density step is used, the most dangerous wavelength λ^* is given by

$$\lambda^* = \frac{\pi}{4}\left\{ g t_2^2 - t_2 \left[g \left(g t_2^2 + \sqrt{3} \cdot 16 A^* \right) \right]^{1/2} + \sqrt{3} \cdot 8 A^* \right\}. \quad (5.16)$$

For A* = 16 μm, 8 μm, and 5 μm the ratios λ^*/A^* are 0.66, 0.35 and 0.23, respectively. In this case, the most dangerous wavelength is even smaller than the critical amplitude. But again the most dangerous wavelength for a density step is considerably smaller than for a gradual density transition (assuming the same shell thicknesses).

5.3.4 Potential effect of reduction of the terminal bubble speed by a gradual density transition

In order to estimate the potential importance of the growth rate reducing effect that a gradual density transition may have during the nonlinear phase in which the bubble grows steadily, one may assume the terminal bubble speed to be given by $F \cdot \sqrt{y^* g \lambda}$. Such a dependence would increase the most dangerous wavelength after either definition by about 30 % and increase the critical initial amplitude by about 40 % (in the cases A* = 16 μm). This rather benign effect is due to the fact that the most dangerous wavelength is about 4 times the length scale L of the density variation anyhow (L = 13.5 μm, A* = 16 μm, λ^* = 52...54 μm) and the effect of the density gradient ceases at $\lambda = 4\pi L$. The latter has been shown to apply

during the linear phase and has been assumed here for the nonlinear phase. But it is clear that there must be a wavelength beyond which a certain density gradient is no longer important. So, one cannot expect another order-of-magnitude effect from a reduction of the terminal bubble speed by a gradual density transition. (It may, however, help considerably when the ratio L/A* is larger.)

5.4 Discussion of effects that could lead to faster instability growth

5.4.1 Effect of finite pusher shell thickness

One difference between the model situation considered here and the real situation in a fusion pellet, which one could consider as important, is the finite thickness of the pusher shell which, in the models from which the growth laws are determined, is replaced by a semi-infinite fluid with constant density.

The linear theory of Rayleigh-Taylor instabilities at finite fluid layers bounded by vacuum on both sides is well established. First Taylor (1950) has considered the case of sinusoidal initial displacements on the two sides which are in phase. Axford (1974) has allowed for a phase shift between these initial displacements and also considered arbitrary initial displacements and certain time-dependent accelerations. Mikaelian (1983a) has generalized Taylor's case by including initial velocity disturbances.

The basic result of all these analyses is that the two surface modes linearly combine to give unstable growth with some superposed oscillations at both interfaces. As shown in subsection 2.3 the growth or oscillation constants of these modes are independent of the density distribution within the fluid. Hence, they are also independent of the fluid layer thickness and this thickness only enters into factors multiplied to the functions describing the growth of the amplitudes. If we take Taylor's case (zero initial velocities) as a typical one and neglect the oscillatory part of the solution, the displacement amplitude h_1 at the unstable surface develops as

$$h_1(t) = \frac{h_{10} - h_{20} \cdot e^{-kd}}{1 - e^{-2kd}} \cosh nt \,. \qquad (5.17)$$

Here h_{10} and h_{20} are the initial displacement amplitudes at the unstable and stable surfaces, respectively, and the minimum pusher shell thickness d has been used as finite fluid layer thickness. One sees (most easily for $h_{20} = 0$) that a disturbance at a finite fluid layer may indeed grow faster than with a semi-infinite fluid. On the other hand, if $h_{20} > h_{10}e^{-kd}$, the disturbance will grow slower than with a semi-infinite fluid. It is, however, more important to realize that the additional factors are quite small and in fact barely realizable as long as $\lambda < \pi d$, say.

The same considerations apply if the unstable free surface is modified by adding a region of exponentially decreasing density. Merely the single unstable free surface mode is replaced by the infinite set of internal modes belonging to the gradual density transition. In the present context the fastest growing mode is the most interesting one (one may even assume only this mode to be present initially) and it will always combine linearly with the oscillatory mode from the stable surface since the eigenfunction of this latter mode is not orthogonal to that of the fastest growing internal mode as those of all the other internal modes are. But, of course, the growth constant of the fastest growing mode depends on the thickness of the fluid layer above the region of exponentially increasing density. Somewhat astonishingly this growth constant slightly decreases when the fluid depth is decreased from infinity to zero. The transcendental equation from which these growth constants can be determined has already been given by Mikaelian (1984).

As to the nonlinear phase, the situation is not as clear. There are some numerical studies available for fluid layers with sharp boundaries but the results are not reported in such a way that they could be used here directly. Verdon et al. (1982) state in their introduction that "For a shell of finite thickness, a constant bubble rise velocity is prohibited by the finite mass reservoir of a fluid layer," and report later that "... the bubble velocity is actually decreasing at the time illustrated, in contrast to the constant bubble rise velocity which results in the semi-infinite layer." It is not clear whether this means that the finite fluid

layer tends to reduce the bubble speed below the terminal bubble speed assumed in the synthetical model. The above cited statements also are possibly not fully in line with what is reported by some of the same authors in McCrory et al. (1981): "The instability evolves because of a nearly constant bubble rise velocity which removes mass from the bubble region," and "... the shell thickness near the bubble decreases linearly with time." (In these calculations the situation may have been different because thermal conduction was included.)

While still not fully conclusive, the reported studies at least do not indicate a sensible increase in the terminal bubble speed due to a finite shell thickness. Furthermore, as derived in the previous subsection, a wavelength about 3 to 4 times the minimum shell thickness should be chosen as the most dangerous one. This is allowed by the results of linear theory presented above and if the final bubble amplitude is only one third of the wavelength, any nonlinear effects should not become too important.

In conclusion, one may state that the effects of a finite fluid layer are negligible at the most interesting wavelengths of 3 to 4 times the layer thickness and that these effects would hardly affect the results derived so far in this chapter.

5.4.2 Effect of compressibility

At the pressure level present during the compression phase (typically several MPa) the pusher material must be considered as compressible in contrast to what has been assumed so far in this report. There has been some confusion about the role that compressibility may play for instability growth. Some of these earlier publications are discussed by Bernstein and Book (1983) and Baker (1983). However, clear and rather general results were first obtained by Kull (1982). For a perfect (polytropic) fluid he showed that the growth constants for unstable modes always increase with compressibility but can never exceed $\sqrt{gk}$. The first part of these findings was also found by Bernstein and Book (1983) for a special case and shown by Newcomb (1983) to be a special case of a known comparison theorem in the calculus of variations. So, this seems to be quite generally valid, shedding some doubt on Baker's (1983) result which includes the

possibility that compressibility decreases the growth constant.

The second part of Kull's (1982) finding makes clear that compressibility has only little effect when the growth constant n is close to $\sqrt{gk}$ anyhow, which has been found confirmed in all the actual cases studied. However, the smaller n is in comparison with $\sqrt{gk}$, the more pronounced is the effect of compressibility. This is found in the special case of a sawtooth-like density profile due to the superposition of two isothermal compressible fluids treated by Kull (1982) and Bernstein and Book (1983). There the reasons for decreasing n are decreasing Atwood ratio and the stabilizing effect of the density gradient outside the unstable interface, which increases with wavelength. So, one might also expect that compressibility can, to some moderate extent, cancel the growth constant reducing effect of a gradual density transition. An evaluation of the importance requires consideration of the special situation and determination of the polytropic exponent that is most suitable to model the pusher material.

For the nonlinear phase, Suydam (1978) presents some arguments leading to the conclusion that the terminal bubble speed will always be well subsonic, so that compressibility may be neglected in this phase.

5.4.3 Effect of three-dimensional disturbances

The synthetical model as presented here consistently assumes two-dimensional disturbances which extend over a distance of at least several wavelengths in the direction perpendicular to the two coordinates here considered. Whether this condition is met in reality must remain an open question. There are, however, indications that three-dimensional disturbances might grow faster. Rajappa and Amaranath (1977) present a nonlinear theory of Rayleigh-Taylor instabilities in three dimensions. Their first-order solution is linear theory. They first compare hexagonal and rectangular disturbance cross-sections and conclude that the rectangular cell pattern will manifest itself because it requires less energy. For the worst case, a quadratic cell and neglecting surface tension, the growth constant is larger than the two-dimensional growth constant by a factor $2^{1/4} \approx 1.189$.

Layzer (1955) has worked out nonlinear models of bubble vertex motion (similar to the one later presented by Kull (1983)) in axially symmetric (cylindrical) and plane two-dimensional flow. For the linear phase he (as later Daly (1969)) finds that the growth constant for cylindrical flow is larger by a factor of $\sqrt{3.832/\pi} \approx 1.104$ where 3.832 stands for the first zero of J_1, the Bessel function of order one.

For the terminal bubble rise the Froude number found by Layzer (1955) for the cylindrical case is even larger by a factor of $\sqrt{3\pi/3.832} \approx 1.568$ so that F = 0.361. This may be compared with F = 0.328 found theoretically (using slightly different approximations) by Davies and Taylor (1950) for bubbles rising in tubes of circular cross-sections if one identifies the wavelength with the tube diameter. Their experimental results vary (essentially with the tube diameter) between 0.283 and 0.346.

Both effects could easily be included into the synthetical model by adjustment of the parameters.

5.4.4 Nonlinear effect of higher harmonics

As shown by Kull (1983) the Froude number F which characterizes the terminal bubble speed depends on the amplitude B of the second harmonic. If one assumes a pure sinusoidal initial perturbation, B = 0 initially. But as shown by the higher-order (nonlinear) theories discussed in 4.4 it starts to grow due to nonlinear effects. In this case the second harmonic is in phase with the fundamental mode so that, after Kull (1983), the Froude number is reduced below its value of 0.236 which it assumes for B = 0. Therefore, F = 0.230 appears to be appropriate for an initially sinusoidal perturbation. If, however, the second harmonic is already present in the initial perturbation, it can occur with a negative initial amplitude (a phase shift of π) and then the Froude number may be larger. This result is confirmed by numerical simulations reported by Verdon et al. (1982). In addition, Baker et al. (1980) have found a similar effect with the fifth harmonic having an initial amplitude one tenths of the initial amplitude of the fundamental mode. They found F to be as high as 0.28 with probably a large error margin. These results show that a larger Froude number may be appropriate if a random distribution of Fourier components in the ini-

tial disturbance is to be taken into account. This can be done easily in the synthetical model.

On the other hand one could speculate that higher harmonics during the linear phase may have a growth reducing effect because they help to create or flatten a density gradient. This occurs at a sharp interface because higher harmonics grow much faster making the interface fuzzy and thus producing a density transition region on the length scale of the basic mode. A similar effect can be expected at a gradual density transition if the length scale L of the density variation is initially much shorter than the minimum shell thickness d. This effect, of course, can only be observed if the most dangerous wavelength itself has to grow by many e-foldings before it can become dangerous.

All in all, the effect of higher harmonics should not be too important. Also, this discussion should cover the nonlinear effect of arbitrary shorter wavelengths, not only just the higher harmonics. The nonlinear effect of larger wavelengths i.e. bubble amalgamation in which faster growing bubbles of larger wavelength "eat up" those of shorter wavelength (see Layzer (1955)) needs not be considered here because it should not become important within the range of amplitudes to be considered.

6. Summary and conclusions

Linear theory of Rayleigh-Taylor instabilities at a region of exponentially increasing density between regions of constant density as developed by Lord Rayleigh (1883) and others is discussed in detail. From this, a simple formula is derived which approximately describes the growth constant reduction by a gradual density transition. It is further shown that an incorrect theory by LeLevier, Lasher, and Bjorklund (1955) underestimates the growth constant.

A simple but effective model of nonlinear bubble growth is obtained from a synthesis of linear theory and constant terminal bubble speed. In its linear part it can take into account the growth constant reduction by a gradual density transition.

The synthetical model of nonlinear bubble growth is applied to the problem of pusher shell breakup in an inertial confinement fusion pellet during the compression phase. The model is used to determine two quantities:

a) maximum allowable initial perturbations
b) most dangerous wavelength.

In the case of a pellet tentatively designed for a conceptual heavy ion-beam driven reactor, the following observations are made (at a wavelength equal to the minimum pusher shell thickness):

a) The gradual density transition at the outside of the pusher shell reduces the growth rate during the linear (small amplitude) regime in such a way that the maximum allowable initial perturbations are increased by a few orders of magnitude.

b) The nonlinear saturation of the bubble growth rate increases the maximum allowable initial perturbations by another order of magnitude.

c) In the presence of the gradual density transition at the outside of the pusher shell, the most dangerous wavelength is about four times the critical amplitude (amplitude at which the pusher shell is broken up) which is usually identified with the minimum pusher shell thickness. In

contrast with that the most dangerous wavelength is about equal to the critical amplitude if the pusher shell is bounded by density steps on both sides.

During ablatively driven compression of an inertial confinement fusion pellet instability growth may be influenced by much more physical processes and boundary conditions than so far considered in the synthetical model. While most of them are expected to further reduce (possibly drastically) instability growth, a few have a potential to accelerate instability growth. In a discussion of these it is found that the finite pusher shell thickness can hardly become important. To some limited extent aggravated growth due to three-dimensional disturbances and nonlinear interaction of higher harmonics present in the initial disturbances could conservatively be accounted for in the synthetical model. But this seems not to be appropriate as long as much more important growth reducing effects are neglected. Compressibility might be the most important growth rate increasing effect. Fortunately its importance increases with decreasing growth constant so that only growth constants far below the classical value can be affected appreciably. It appears that this effect should be accounted for in a more complete theory. To this end, studies of the special density profile and the material properties are required.

The above considerations suggest that the synthetical model and the approximate formula to account for a gradual density transition, which both are reasonably conservative in the model situations from which they were obtained may allow a conservative estimate of instability growth during pellet compression. However, use of these results to determine whether the pusher shell in a certain case will be destroyed by Rayleigh-Taylor instabilities is counterindicated by at least two reasons: In the first place, the model most probably is overly pessimistic because several effects are not yet included, which have the potential of effectively reducing instability growth. Secondly, knowledge on the effective initial perturbations within the instability zone is still insufficient. The model can rather serve to determine a figure of merit such as the maximum allowable initial perturbation, which allows to compare different pellet designs and/or illumination histories with respect to Rayleigh-Taylor instability growth.

As a consequence of the findings with respect to the most dangerous wavelength and the (small) effect of the finite pusher shell thickness, a wavelength about three to four times as long as the critical amplitude may be chosen when determining the figure of merit. This reduces the importance of nonlinear effects within the amplitude range to be considered.

An outline is given of how the synthetical model could be made more realistic and flexible and slightly more complete using already available numerical techniques and numerical results from a pellet simulation code. Also, the nonlinear theories presently available in the literature are briefly discussed.

7. Literature

Amaranath, T. and N.R. Rajappa, 1976, Acta Mechanica 24, 87-97

Amaranath, T., 1980, Acta Mechanica 37, 169-177

Axford, R.A., 1974, "Initial Value Problems of the Rayleigh-Taylor Instability Type", Report LA-5378, Los Alamos Scientific Laboratory

Baker, G.R., D.I. Meiron, and S.A. Orszag, 1980, Phys Fluids 23, 1485-1490

Baker, L. and J.R. Freeman, 1981, J Appl Phys 52, 655-663

Baker, L., 1983, Phys Fluids 26, 950-952

Bangerter, R.O., J.D. Lindl, C.E. Max, and W.C. Mead, 1975, Proc. 1st Int. Top. Conf. Electron Beam Research and Technology, Albuquerque, NM, Nov. 3-5, Report SAND76-5122, Sandia Laboratories, Albuquerque, pp. 15-36

Bangerter, R.O. and D.J. Meeker, 1977, Proc. 2nd Int. Top. Conf. High Power Electron Beam Research and Technology, October 3-5, 1977, Ithaca, NY, pp. 183-193

Batchelor, G.K., 1967, "An Introduction to Fluid Dynamics", Cambridge University Press, Cambridge

Bernstein, I.B. and D.L. Book, 1983, Phys Fluids 26, 453-458

Birkhoff, G.B., 1955, "Taylor Instability and Laminar Mixing", Report LA-1862, Los Alamos Scientific Laboratory

Birkhoff, G. and D. Carter, 1957, J Math Mech 6, 769-779

Book, D.L. and I.B. Bernstein, 1980, J Plasma Phys 23, 521-533

Buchwald, G., H. Kruse, J. Theis, J.A. Maruhn, and H. Stöcker, 1982, Proc. Symp. Accelerator Aspects of Heavy Ion Fusion, Darmstadt, Report GSI-82-8, Gesellschaft für Schwerionenforschung, Darmstadt, pp. 585-597

Capriotti, E.R., 1973, Astrophys J 179, 495-516

Case, K.M., 1960, in "Hydrodynamic Instability", Proc. of the 13th Symp. in Applied Mathematics of the American Mathematical Society, New York, NY, April 14-15, pp. 25-33

Chakraborty, B.B., 1975, Phys Fluids 18, 1066-1067

Chandrasekhar, S., 1961, "Hydrodynamic and Hydromagnetic Stability", Dover Publications, New York

Crowley, W.P., 1970, "An Empirical Theory for Large Amplitude Rayleigh-Taylor Instability", Report UCRL-72650, Lawrence Radiation Laboratory, Livermore

Daly, B.J., 1967, Phys Fluids 10, 297-307

Daly, B.J., 1969, Phys Fluids 12, 1340-1354

Dienes, J.K., 1978, Phys Fluids 21, 736-744

Emmons, H.W., C.T. Chang and B.C. Watson, 1960, J Fluid Mech 7, 177-193

Fishburn, B.D., 1974, Acta Astronautica 1, 1267-1284

Frese, M.H., 1982, Bull Am Phys Soc 27, 964 (in abstract form only)

Frieman, E.A., 1954, Astrophys J 120, 18-21

Fröhlich, G., and M. Anderle, 1980, "Experimente zum Studium der Auslösemechanismen für Wasserdampfexplosionen", Report IKE 2-51, Inst. f. Kernenergetik und Energiesysteme, Universität Stuttgart

Gamalii, E.G., V.B. Rozanov, A.A. Samarskii, V.F. Tishkin, N.N. Tyurina, and A.P. Favorskii, 1980, Sov Phys JETP 52, 230-237

Garabedian, P.R., 1957, Proc Roy Soc A241, 423-431

Gerhauser, H., 1980, "Theoretische Analyse des turbulenten Transports durch die diffuse Grenzschicht bei der dynamischen Stabilisierung überschichteter mischbarer Flüssigkeiten", Report Jül-1645, Kernforschungsanlage Jülich

Gerhauser, H., 1983, "Hydrodynamic Theory of Convective Transport Across a Dynamically Stabilized Diffuse Boundary Layer", Report Jül-1869, Kernforschungsanlage Jülich

Harlow, F.H. and J.E. Welch, 1966, Phys Fluids 9, 842-851

Hendricks, C.D., J.K. Crane, E.J. Hsieh and S.F. Meyer, 1981, Thin Solid Films 83, 61-72

Hunt, J.N., 1961, Appl Sci Res A 10, 45-58

Hussey, T.W. and D.H. McDaniel, 1981, Comments Plasma Phys Cont Fusion 6, 177-185

Ince, E.L., 1926, "Ordinary Differential Equations", reprinted by Dover Publications, New York, 1956

Ingraham, R.L., 1954, Proc Phys Soc 67B, 748-752

Jacobs, H., 1983, in "Studies on the Feasibility of Heavy Ion Beams for Inertial Confinement Fusion", Annual Report 1982, Report GSI-83-2, Gesellschaft für Schwerionenforschung, Darmstadt, p. 46

Kiang, R.L., 1969, Phys Fluids 12, 1333-1339

Kidder, R.E., 1976, Nuclear Fusion 16, 3-14

Kull, H.J., 1982, "Perfect Fluid Model of Rayleigh-Taylor Instability", IAP-Report 102/82, Inst. f. Angewandte Physik, Technische Hochschule Darmstadt

Kull, H.J., 1983, Phys Rev Lett 51, 1434-1437

Lamb, H., 1911, Proc Roy Soc A84, 551-572

Lamb, Sir Horace, 1932, "Hydrodynamics", 6th Ed., at the University Press, Cambridge, reprinted by Dover Publications, New York, 1945

Layzer, D., 1955, Astrophys J 122, 1-12

LeLevier, R., G.J. Lasher, and F. Bjorklund, 1955, "Effect of a Density Gradient on Taylor Instability", Report UCRL-4459, Radiation Laboratory, Livermore

Lewis, D.J., 1950, Proc Roy Soc A202, 81-96

McCrory, R.L., L. Montierth, R.L. Morse, and C.P. Verdon, 1981, Phys Rev Lett 46, 336-339

Menikoff, R., R.C. Mjolsness, D.H. Sharp, C. Zemach, and B.J. Doyle, 1978, Phys Fluids 21, 1674-1687

Menikoff, R. and C. Zemach, 1983, J Comp Phys 51, 28-64

Mikaelian, K.O., 1982, Phys Rev A 26, 2140-2158

Mikaelian, K.O., 1983a, Phys Rev A 28, 1637-1646

Mikaelian, K.O., 1983b, Phys Lett 99A, 46-50

Mikaelian, K.O. and J.D. Lindl, 1984, Phys Rev A 29, 290-296

Nayfeh, A.H., 1969, J Fluid Mech 38, 619-631

Pert, G.J., 1981, in "Plasma Physics and Nuclear Fusion Research", Academic Press, London, pp. 571-597

Pilch, M., C.A. Erdman, and A.B. Reynolds, 1981, "Acceleration Induced Fragmentation of Liquid Drops", Report NUREG/CR-2247, Department of Nuclear Engineering, University of Virginia, Charlottesville

Plesset, M.S. and R.B. Chapman, 1971, J Fluid Mech 47, 283-290

Prosperetti, A., 1981, Phys Fluids 24, 1217-1223

Prosperetti, A. and J.W. Jacobs, 1983, J Comp Phys 51, 365-386

Rajappa, N.R., 1967, "A Non-linear Theory of Taylor Instability of Superposed Fluids", PhD Thesis, Stanford University, see also: Rajappa, N.R. and I.D. Chang, 1966, "Surface Tension Effects on the Motion of a Bubble and Spike Generated by Taylor Instability", Dept of Aeronautics and Astronautics, Stanford University, Report No. 286

Rajappa, N.R., 1970a, J Phys Soc Japan 28, 219-224

Rajappa, N.R., 1970b, Acta Mechanica 10, 193-205

Rajappa, N.R. and T. Amaranath, 1977, Q Jl Mech appl Math 30, 131-141
See also corrigendum, Q Jl Mech appl Math 32 (1979) 93

Rayleigh, Lord, 1883, Proc London Math Soc 14, 170-177, reprinted in "Scientific Papers", Cambridge U.P., 1900, Vol. II, p. 200 (again reprinted by Dover Publications, New York, 1965)

Richtmyer, R.D., 1960, Comm Pure Appl Math 13, 297-319

Ripin, B., S.E. Bodner, P.G. Burkhalter, H. Griem, J. Grun, H. Hellfeld, M.J. Herbst, R.H. Lehmberg, C.K. Manka, E.A. McLean, S.P. Obenschain, J.A. Stamper, R.R. Whitlock, F.C. Young, 1982, "Plasma Physics and Controlled Nuclear Fusion Research 1982", Ninth Conf. Proc., Baltimore, Nuclear Fusion, Supplement 1983, Vol. I, pp. 139-154

Suydam, B.R., 1978, "Breakup of an Accelerated Shell Owing to Rayleigh-Taylor Instability", Report LA-7291-MS, Los Alamos Scientific Laboratory

Tahir, N.A. and K.A. Long, 1982, Atomenergie/Kerntechnik 40, 157-170

Targove, J.D., 1981, "A Variational Approach to the Rayleigh-Taylor Instability of an Accelerating Plasma Slab", Thesis, AD-A-118074 NTIS

Taylor, Sir Geoffrey, 1950, Proc Roy Soc A201, 192-196

Verdon, C.P., R.L. McCrory, R.L. Morse, G.R. Baker, D.I. Meiron, and S.A. Orszag, 1982, Phys Fluids 25, 1653-1674